

New Phytologist

Tibetan meadow degradation alters resource exchange currency, network complexity, and biomass allocation tradeoff of arbuscular mycorrhizal symbiosis

Journal:	<i>New Phytologist</i>
Manuscript ID	NPH-MS-2024-46493
Manuscript Type:	Full Paper
Date Submitted by the Author:	03-Mar-2024
Complete List of Authors:	Gao, Cheng; Institute of Microbiology Chinese Academy of Sciences, State Key Laboratory of Mycology Dong, Qiang; Institute of Microbiology Chinese Academy of Sciences, State Key Laboratory of Mycology Ren, ShiJie; Beijing Forestry University, School of Grassland Science Li, Yaoming; Beijing Forestry University, School of Grassland Science Ji, Baoming; Beijing Forestry University, School of Grassland Science Willing, Claire; University of Washington, School of Environmental and Forest Sciences Adams, Catharine; University of California Berkeley, Department of Plant and Microbial Biology
Key Words:	arbuscular mycorrhizal fungi, resource exchange currency, network, biomass allocation, Tibetan alpine meadow, degradation

SCHOLARONE™
Manuscripts

1 **Tibetan meadow degradation alters resource exchange currency, network**
2 **complexity, and biomass allocation tradeoff of arbuscular mycorrhizal symbiosis**

3

4 Qiang Dong^{1,2}, Shi-Jie Ren², Claire Elizabeth Willing³, Catharine Allyssa Adams^{4,5}, Yao-
5 Ming Li², Bao-Ming Ji^{2*}, Cheng Gao^{1,6*}

6 ¹ State Key Laboratory of Mycology, Institute of Microbiology, Chinese Academy of
7 Sciences, Beijing 100101, China

8 ² School of Grassland Science, Beijing Forestry University, Beijing 100083, China

9 ³ School of Environmental and Forest Science, University of Washington, Seattle, WA
10 98195, USA

11 ⁴ Department of Plant and Microbial Biology, University of California, Berkeley, CA
12 94720-3102, USA

13 ⁵ Environmental Genomics and Systems Biology Division, Lawrence Berkeley National
14 Laboratory, Berkeley, CA 94720, USA

15 ⁶ College of Life Sciences, University of Chinese Academy of Sciences, Beijing 100049,
16 China

17

18 * Correspondence:

19 Bao-Ming Ji, e-mail: baomingji@bjfu.edu.cn

20 Cheng Gao, e-mail: gaoc@im.ac.cn

21

22 **ORCIDs**

23 Cheng Gao <https://orcid.org/0000-0003-2522-7909>

24 Qiang Dong <https://orcid.org/0009-0001-3875-329X>

25 Shi-Jie Ren <https://orcid.org/0009-0008-8577-3294>

26 Claire Elizabeth Willing <https://orcid.org/0000-0002-7563-242X>

27 Catharine Allyssa Adams <https://orcid.org/0000-0002-0914-0806>

28 Yao-Ming Li <https://orcid.org/0000-0002-7892-6300>

29 Bao-Ming Ji <https://orcid.org/0000-0002-8333-5978>

30 **Summary**

31 The response of arbuscular mycorrhizal (AM) symbiosis to environmental fluctuations
32 involves complex interactions between host plants and fungal partners, between
33 different AM fungal members, and between AM fungal vegetative or reproductive
34 structures; yet a systematic understanding of these responses to meadow degradation
35 remains relatively unknown, particularly in Tibetan meadow. Here, we approached this
36 knowledge gap by labeling dual isotopes of air $^{13}\text{CO}_2$ and soil $^{15}\text{NH}_4\text{Cl}$, computing
37 ecological network of AM fungal community, and quantifying AM fungal biomass
38 allocation among reproductive spore, and vegetative intra- and extra-radical hyphae.
39 We found that the exchange currency of photosynthate and nitrogen between plants
40 and AM fungi was increased with increasing severity of meadow degradation,
41 indicating greater dependence of host plant on this symbiosis for resource acquisition.
42 Besides, using 18S rRNA amplicon sequencing, we found that AM fungal co-occurrence
43 networks were complexified by meadow degradation, supporting the stress gradient
44 hypothesis. Meadow degradation also increased AM fungal biomass allocation toward
45 traits associated with resource acquisition (intra- and extra-radical hyphae) at the
46 expense of reproductive spores. Our findings suggest that an integrated consideration
47 of resource exchange, ecological networks and biomass allocation may be important
48 for the restoration of degraded ecosystems.

49

50 **Keywords:** arbuscular mycorrhizal fungi, resource exchange currency, network,
51 biomass allocation, Tibetan alpine meadow, degradation

52

53 Introduction

54 The Anthropocene has witnessed significant degradation of grasslands, along with
55 declines in biodiversity and ecosystem services (Gibbs & Salmon, 2015; Bardgett *et al.*,
56 2021; Bai & Cotrufo, 2022). Alpine meadows are especially sensitive to degradation
57 caused by anthropogenic activities and climate change due to the short growing
58 seasons and often slow growth strategies of many of the local biota (Dong *et al.*, 2020;
59 Breidenbach *et al.*, 2022). The Tibetan Plateau, the largest high-altitude meadow
60 system in the world, plays an essential role in water storage for local ecology and
61 human populations (Bai & Cotrufo, 2022; Zhu *et al.*, 2023). However, as a result of
62 overgrazing, exotic species invasion, and climate change-induced warming and
63 drought, approximately 90% of the Tibetan Plateau is considered degraded (Harris,
64 2010). These degraded alpine meadows are characterized by a reduction in plant cover,
65 nitrogen (N) availability, soil erosion, and substantial nutrient losses (Breidenbach *et*
66 *al.*, 2022; Li *et al.*, 2022), potentially further exacerbating the sensitivity of these
67 systems to future disturbance.

68 To cope with these environmental perturbations like those in this meadow system,
69 plants often enlist microbial partners (de Vries *et al.*, 2020; Coban *et al.*, 2022). In
70 particular, root-associated mutualists known as arbuscular mycorrhizal (AM) fungi can
71 play an outsized role in the stability and functioning of grassland systems (Smith &
72 Read, 2008; Davison *et al.*, 2015; Vetrovsky *et al.*, 2023). These fungi can increase plant
73 access to limiting soil nutrients (Hodge *et al.*, 2010) and water (Kakouridis *et al.*, 2022).
74 The response and functioning of arbuscular mycorrhiza to grassland degradation may
75 involve the interaction between the host plant and AM fungal partner, the interaction
76 between different AM fungal taxa, and the biomass allocation among AM fungal
77 vegetative and reproductive structures. Thus, a thorough understanding of the
78 response and function of AM symbiosis to grassland degradation is important for the
79 sustainability of the Tibetan Plateau.

80 The stability of plant-AM fungal symbiosis depends on cooperation of both
81 partners, where the fungus provides the plant with access to limiting nutrients, while

82 the plant supplies the fungal partner with photosynthate (Kiers *et al.*, 2011). Biological
83 market theory posits that the reciprocal regulation of these “goods” between the host
84 plant and AM fungi is essential for the maintenance and prosperity of AM symbiosis
85 (Selosse & Rousset, 2011; Bennett & Groten, 2022; Martin & van der Heijden, 2024).
86 For example, fostered by dual-labeling of carbon (C) and N isotopes, several previous
87 studies have found that the currency in exchanging plant-derived C for AM fungi-
88 derived N was variable with the identity of AM fungal taxa (Arguello *et al.*, 2016), soil
89 nutrient availability (Liu *et al.*, 2021), plant development stage (Tome *et al.*, 2015), and
90 atmospheric CO₂ concentrations (Tome *et al.*, 2015; Zhang *et al.*, 2015; Charters *et al.*,
91 2020) (Table S1). The degradation of grassland is often coupled with a reduction in N
92 availability and an increase in harsh environmental conditions, due to heavy soil
93 erosion and substantial nutrient losses (Breidenbach *et al.*, 2022; Li *et al.*, 2022). In the
94 context of our system, plants in degraded alpine meadows must cope with declines in
95 N availability, which may shift “market” exchange rates for plant-fungal partners.
96 Thereby, we hypothesize H₁ that the currency in exchanging plant C for AM fungal N
97 will be higher in the degraded meadow than in the non-degraded meadow.

98 In addition to the reciprocal regulation between plant and AM fungi, the
99 response of AM symbiosis to meadow degradation may also involve the interaction
100 with different members of the AM fungal community, which may be depicted by the
101 complexity of co-occurrence network. Our hypothesis in this area is guided by the
102 stress gradient hypothesis (Brooker *et al.*, 2007; Hammarlund & Harcombe, 2019),
103 which posits that positive associations should increase in frequency under stress.
104 Several recent studies found that the positive associations of fungal and bacterial
105 communities were increased by stress caused by drought, degradation, and
106 elevation/water availability (Che *et al.*, 2019; Hernandez *et al.*, 2021; Gao *et al.*, 2022).
107 However, to our knowledge, how the associations among AM fungal taxa response to
108 meadow degradation remains unknown. Here, guided by the stress gradient
109 hypothesis and considering the increase of resource scarcity and environmental
110 harshness in degraded meadow, we hypothesize that H₂, the complexity of co-

111 occurrence network increases in degraded meadow compared to non-degraded
112 meadow.

113 The functioning of arbuscular mycorrhiza is eventually defined by the biomass
114 allocation among three typical morphological structures, i.e., intraradical hyphae
115 (arbuscule, vesicles and coils), extraradical hyphae, and asexual spores (Choi *et al.*,
116 2018; Chaudhary *et al.*, 2022). Extraradical hyphae are responsible for accessing critical
117 inorganic nutrients from the soil matrix, intraradical hyphae (e.g. arbuscules) form the
118 interface for the exchange of these inorganic nutrients and plant photosynthates, and
119 dormant asexual spores are important propagules for AM fungal colonization and
120 dispersal that represent an important survival strategy under adverse environmental
121 conditions (Chagnon *et al.*, 2012; Chaudhary *et al.*, 2022) (Table S2). A recent study in
122 wheat field found that the ratio of AM fungal extraradical hyphal density (ERHD) to
123 intraradical colonization rate (IRCR) was decreased significantly with N fertilization
124 (Babalola *et al.*, 2022). However, few studies have investigated how meadow
125 degradation may impact AM fungal biomass allocation to growth versus reproduction
126 (Tian *et al.*, 2009; Mao *et al.*, 2019). Under resource limitation, trait tradeoffs theories
127 for microbes suggest that traits associated with stress tolerance and resource
128 acquisition would be upregulated (Malik *et al.*, 2020; Wang *et al.*, 2023). For example,
129 AM fungi would be more likely to invest in traits associated with resource acquisition
130 such as (intra- and extra-radical) hyphal growth to improve C for nutrient exchange
131 with host plants, this would come at the cost of fungal spore production. Besides, in
132 adapting to the stressed degraded meadow, dormant AM fungal spores may germinate
133 to active (intra- and extra-radical) hyphae to improve the nutrient condition of the host,
134 as a result depleting the soil spore pool. Therefore, we hypothesize H₃, that
135 degradation increases AM fungal biomass allocation to vegetative hyphae at the
136 expense of reproductive spore.

137 Here, we test these three hypotheses along a meadow degradation gradient in
138 the Tibetan Plateau (Fig. S1), by blending ¹³C and ¹⁵N isotope labeling, 18S rRNA gene
139 amplicon sequencing, and morphological examination. Our H₁ (degradation increases

at the community level

140 the currency in exchanging plant C for AM fungal N) was supported by the finding that
141 the ratio of $^{13}\text{C}:^{15}\text{N}$ increased from non-degraded, through moderately degraded, to
142 severely degraded meadow. The H₂ (degradation increases network complexity) was
143 supported by the finding that the complexity of the AM fungal co-occurrence network
144 increased from non-degraded, through moderately degraded, to severely degraded
145 meadow. The H₃ (degradation increases AM investment in nutrient acquisition at the
146 cost of reproduction) was supported as that meadow degradation significantly
147 decreased AM fungal reproductive spore density (SD), but increased vegetative intra-
148 and extra-radical hyphal density.

150 Results and discussion

151 Before hypotheses testing, we measured vegetation and soil variables in the non-
152 degraded, moderately degraded and severely degraded meadows (Fig. S1). The results
153 showed that plant aboveground biomass, plant belowground biomass, plant species
154 richness, plant coverage and soil available phosphorus (AP), ammonium-nitrogen
155 ($\text{NH}_4^+\text{-N}$), nitrate-nitrogen ($\text{NO}_3^-\text{-N}$), soil organic carbon (SOC), total nitrogen (TN),
156 easily extractable glomalin-related soil protein (EE-GRSP) and total glomalin-related
157 soil protein (T-GRSP) were all decreased by meadow degradation (Fig. S2-3).

158 **AM fungal community characterization:** AM fungal community was characterized
159 from root and soil samples collected from the same non-degraded, moderately
160 degraded and severely degraded meadows using 18S rRNA metabarcoding amplicon
161 sequencing. Our analysis detected 115 AM fungal operational taxonomical units (OTUs)
162 dominated by *Glomus*, *Claroideoglomus* and *Rhizophagus* (Fig. 1a; Fig. S4-6). Principal
163 coordinate (PCo) analysis detected significant associations of AM fungal community
164 composition with compartment (root v.s. soil), degradation stage (non-, moderately,
165 or severely), and their interaction (Fig. 1b). The effects of compartment and meadow
166 degradation on AM fungal community is complemented with the detection of 16 AM
167 fungal OTUs significantly biased in the three meadow degradation stages and two
168 compartments (Fig. 1c-d; Fig. S7). Furthermore, the Bray-Curtis dissimilarity of AM

169 fungal community between root and soil was increased significantly by meadow
170 degradation (Fig. 1e), suggesting increases of niche differentiation between root and
171 soil AM fungal community. Meanwhile, meadow degradation caused the dispersion in
172 beta diversity of AM fungal community in root but not in soil (Fig. 1f).

173

174 **Testing H₁: Meadow degradation increases the currency in exchanging plant-derived** 175 **C for AM fungi-derived N**

176 To test our H₁ that meadow degradation increases the currency in exchanging plant C
177 for AM fungal N, we performed a greenhouse experiment of meadow plants growing
178 on soil collected from the non-degraded, moderately degraded and severely degraded
179 meadow (Fig. S1). The system was dual labeled with ¹³CO₂ (air chamber) and ¹⁵NH₄Cl
180 (in-growth bottle) 94 days after the seedling was planted (Fig. 2a-b), and harvested
181 three days later. We measured the concentration of ¹⁵N in each individual plant and
182 the concentration of ¹³C in AM fungal biomass, via phospholipid fatty acid (PLFA)
183 analysis (Olsson *et al.*, 1995). The currency of resource exchange is depicted by the
184 ratio of AM fungal ¹³C: plant ¹⁵N (C: N).

185 We found that the concentration of ¹³C detected in AM fungal hyphae was
186 significantly lower in non-degraded meadow as compared to the moderately and
187 severely degraded meadows (Fig. 2c), whereas the concentration of ¹⁵N detected in
188 plants was not significantly affected by meadow degradation (Fig. 2d). As a result, the
189 resource exchange currency as depicted by the ratio of ¹³C: ¹⁵N was significantly higher
190 in the moderately and severely degraded meadows, as compared to that in the non-
191 degraded meadow (Fig. 2e).

192 Our dual isotopes label-based research supports H₁, as degradation increased the
193 currency in the exchange of plant photosynthate and AM fungal absorbed N (Fig. 2).
194 The detected increase in C: N currency exchange is not due to the reduction of
195 resource availability in the severely degraded meadow, as the same substrate was
196 used in our greenhouse-based dual isotope research. Because our system was
197 inoculated with AM fungal community derived from soil of different degradation

198 levels, our finding suggests that the variation in AM fungal community structure might
199 be responsible for the increase in the currency of C: N exchange with increasing
200 intensity of meadow degradation.

201 Our study built on previous studies that used a single AM fungal species, by using
202 an AM fungal community to investigate the currency of resource exchange between
203 plants and AM fungi. For example, a previous study suggested that the currency in the
204 exchange between plant C and AM fungal N can vary with the identities of plant and
205 AM fungi (*Funneliformis mosseae* or *Rhizophagus intraradices*) that are involved in the
206 formation of common mycorrhizal networks in a compartmentalized pot system in a
207 greenhouse (Walder *et al.*, 2012). Furthermore, a positive correlation between a plant
208 photosynthetic rate and the hyphal N absorption capacity of two AM fungal species
209 (*F. mosseae* and *R. intraradices*) has been implied in a compartmented pot system
210 (Tome *et al.*, 2015). To our knowledge, we are the first to show that the currency in
211 exchanging C and N between plant and AM fungi is increased by inoculation of AM
212 fungal community from the soil with increasing intensity of degradation. Our finding
213 suggests a greater dependence of host plant on AM symbiosis for resource acquisition
214 in degraded meadow, and this conditioned might be harnessed for the resistance,
215 resilience, and restoration of Tibetan meadow.

216

217 **Testing H₂: Meadow degradation increases network complexity**

218 Our H₂ was tested by computing the pairwise Spearman correlations among AM fungal
219 OTUs in each meadow degradation level. The distribution density curve of all-
220 correlations (both significant and non-significant) showed that the proportion of
221 positive correlations was significantly higher in the severely and moderately degraded
222 meadows, as compared to the non-degraded meadow (Fig. S8-9). We found support
223 for the stress gradient hypothesis because meadow degradation increased the relative
224 frequency of positive correlations among AM fungal taxa (Fig. S8-9).

225 Our co-occurrence network analysis showed that meadow degradation increased
226 the complexity of the AM fungal network from non-degraded meadow, through

227 moderately to severely degraded meadow, as evidenced by the doubling of edge
228 number, connectivity, average degree and average clustering coefficient, and
229 increasing dominance of *Glomus* taxa (Fig. 3d-h). Specifically, the number of significant
230 positive correlations doubled in the severe degraded meadow as compared to the
231 non-degraded meadow (Fig. 3). Note, in our system, the number of positive
232 associations was highest in resource poor (low in N and phosphorus availability),
233 severely degraded meadow; however, a recent study found that positive associations
234 were highest in grassland receiving the highest amount of N input (Wu *et al.*, 2022).
235 Due to the huge difference in experiment design (degradation v.s. N addition),
236 ecosystem type (alpine meadow v.s. temperate grassland), and sampling types (root +
237 soil v.s. soil only) and the complex function that AM fungi perform with respect to
238 resource absorption, how the AM fungal community might respond to environmental
239 changes remains to be investigated. Our finding suggests more cooperation among AM
240 fungal taxa in degraded meadow, which may be essential for resource scavenge and
241 stress resistance in degraded meadow.

242
243 **Testing H₃: Meadow degradation increases AM fungal biomass allocation to hyphae**
244 **at the expense of spore.**

245 To test our H₃, we measured root AM fungal IRCR and soil ERHD and SD, and calculated
246 the ratios between IRCR: ERHD, IRCR: SD, and ERHD: SD. Our analysis supports the H₃,
247 as degradation increased AM fungal biomass allocation to hyphae at the expense of
248 spore (Fig. 4). Specifically, in the severely degraded meadow as compared to the non-
249 degraded meadow, AM fungal ERHD and IRCR roughly doubled, whereas AM fungal
250 soil SD roughly halved (Fig. 4b, c). As a result, with a stable ERHD: IRCR ratio, both the
251 SD: ERHD and SD: IRCR dropped with increasing degradation level (Fig. 4d-f). Our
252 findings in Tibetan meadow are partially supported by a previous study in Inner
253 Mongolia grassland. Tian *et al* found grazing-induced degradation decreased AM
254 fungal SD and increased or decreased IRCR depending on the identity of the plant
255 species (Tian *et al.*, 2009). In addition, another study along a transect from Tibetan

256 meadow to steppe found that topsoil removal-induced degradation decreased ERHD
257 and SD but increased IRCR (Mao *et al.*, 2019). However, neither study captured the
258 signal of AM fungal biomass allocation, because the SD: IRCR, SD: ERHD and ERHD:
259 IRCR ratios were not calculated. Together, our current work and certain previous
260 studies confirm that habitat degradation induces changes in AM fungal biomass
261 allocation, though the precise patterns of changes may differ with ecosystem and
262 degradation type. Our finding showed that meadow degradation increased AM fungal
263 biomass allocation to hyphae at the expense of spore, indicating that restoration of
264 degraded meadow might be accelerated by exogenous additions of AM fungal spores.

266 **Conclusion**

267 We detected a systematic response of AM symbiosis to meadow degradation, by
268 showing an increase in the exchange currency between plant C and AM fungal N, an
269 increase in the complexity of AM fungal co-occurrence network and an increase in AM
270 biomass allocation toward hyphae at the expense of spores. Our ability to detect this
271 systematic response largely relies on blending techniques of dual isotope labeling, 18S
272 rRNA gene amplicon sequencing, and morphological examination. Our finding is
273 important because Tibetan meadow is one of the most fragile yet essential ecosystems
274 on the planet, and we found that AM symbiosis is more than only responsive and may
275 be essential to the restoration of meadow degradation.

277 **Materials and Methods**

278 Our research site was located at the Naqu Ecological and Environmental Observation
279 and Research Station (31°16'N, 92°06'E, 4500 m above sea level, mean annual
280 temperature of -2.1 °C, mean annual precipitation of 406 mm), a distribution center of
281 *Kobresia pygmaea*, the iconic plant species of the Tibetan alpine meadow ecosystem
282 (Li *et al.*, 2016). Our research used 18 total plots of non-degraded (6 plots), moderately
283 degraded (6 plots), and severely degraded (6 plots) meadows previously established
284 by Li *et al.* (2016) (Fig. S1). Briefly, six replication plots, each 5 m × 5 m, and at least 20

285 m away from each other were randomly selected for each degradation level. The non-
286 degraded meadow was intact turf with >90% canopy coverage dominated by *Kobresia*
287 *pygmaea*; the moderately degraded meadow was patched turf with ~40% coverage by
288 *Kobresia pygmaea* accompanied with crusts of Cryptogams; the severely degraded
289 meadow was deserialized turf dominated by forbs (e.g. *Lancea tibetica*) (Fig. S1). In
290 July 2018, a vegetation survey and sampling of roots and soil were performed in each
291 plot. Plant community coverage, species identity, richness and composition were
292 measured using point-intercept sampling with a 50 cm × 50 cm square frame.
293 Subsequently, plant aboveground biomass was collected by clipping each plant at the
294 soil surface, and plant belowground biomass was collected from two soil cores
295 (diameter 5 cm, depth 20 cm), both of which were then dried at 60 °C for 48 hours.

296 At each quadrat, five soil cores were collected randomly and mixed into one
297 sample. Soil samples were sifted through a 2-mm mesh sieve, the recovered roots
298 were washed with distilled water. The root and soil samples were immediately packed
299 in an ice box and transported to the laboratory. Root samples and soil subsamples
300 were stored at -20 °C for DNA extraction and measurements of AM fungal IRCR and
301 ERHD. Fresh soil subsamples were used to measure soil AP, NH₄⁺-N, NO₃⁻-N, pH and for
302 the mycorrhizal inoculation experiment. The other portion of each soil sample was air-
303 dried to measure SOC, TN, TP, AM fungal SD, EE-GRSP and T-GRSP. Five dominant and
304 companion plant individuals were selected randomly from each quadrat and pooled
305 as one sample to store at -20 °C for DNA extraction. In total, 72 samples were collected
306 (three degradation stages × four types of samples (soil + mixed root + dominant plant
307 + companion plant) × six replicates).

308 Soil AP and TP were extracted with NaHCO₃ and KClO₄-H₂SO₄ respectively, and
309 then quantified with the Mo-Sb colorimetric method (Bray & Kurtz, 1945; Bowman,
310 1988). Soil NH₄⁺-N was measured by the indophenol blue method (Dorich & Nelson,
311 1983), and NO₃⁻-N was measured with a UV spectrophotometer at wavelengths 270
312 nm and 210 nm (Norman *et al.*, 1985). Soil TN was determined by the Kjeldahl method
313 (Davidson *et al.*, 1970). SOC was estimated by the potassium dichromate titrimetric

314 method (Sims & Haby, 1971). Soil pH was measured in a 1:2.5 (w/v) soil-to-water
315 suspension with a pH meter. EE-GRSP and T-GRSP were determined by the procedures
316 reported by Wright and Upadhyaya (1996).

317 AM fungal spores were extracted from 50.0 g of air-dried soil by wet sieving
318 (bottom 38 µm mesh) and the sucrose centrifugation method (Brundrett *et al.*, 1994).
319 The extraradical hyphae were extracted from 5.0 g of frozen soil using a membrane
320 filter, stained with Trypan blue and examined using the grid line intersection method
321 under ×200 magnification by observing 25 random fields of view (Brundrett *et al.*,
322 1994). The plant roots were washed carefully and cut into 1-cm fragments, treated
323 with 10% KOH at 90 °C for 30 min, and acidified in 2% HCl at room temperature for 10
324 min, followed by staining with 0.05% Trypan blue at 90 °C for 10 min. Finally, 100 dyed
325 root segments were randomly selected and measured for AM fungal colonization by
326 the grid line intersection method under ×200 magnification (Mcgonigle *et al.*, 1990).

327 The DNA was extracted from 0.1 g fine roots and 0.5 g soil using the Powerplant
328 and Powersoil DNA Isolation Kits (MoBio Laboratories, USA), respectively. To amplify
329 the 18S rRNA gene, a two-step polymerase chain reaction (PCR) was performed using
330 the NS31/AML2 primer pair (Lumini *et al.*, 2010) and AMDGR/AMV4.5NF (with 12-base
331 barcode sequences) primer pair (Sato *et al.*, 2005; Van Geel *et al.*, 2014), using the PCR
332 conditions described by Dong *et al.* (2021). The PCR products were purified with an
333 agarose gel DNA purification kit (AP-GX-250G; Axygen, United States) and quantified
334 using a NanoDrop 8000 (NanoDrop Technologies, Wilmington, DE, USA), then pooled
335 together with the same molar amount (100 ng) from each sample and sequenced on
336 the Illumina MiSeq PE250 platform at Chengdu Institute of Biology, Chinese Academy
337 of Sciences, China. The sequences obtained in this study were submitted to the
338 GenBank database (PRJNA1060898).

339 The raw sequence was subjected to quality control using Quantitative Insights
340 Into Microbial Ecology (QIIME v1.7.0), and the obtained high-quality sequences were
341 imported into USEARCH v11.0 for dereplication, and chimeras were detected and
342 removed (Caporaso *et al.*, 2010; Edgar, 2013). All non-chimeric sequences were

343 clustered into OTUs at a 97% similarity level. The representative sequences of OTUs
344 were uploaded to the National Center for Biotechnology Information (NCBI) and the
345 MarrjAM database (Opik *et al.*, 2010) for taxonomic identification. The phylogenetic
346 tree of AM fungal OTUs was constructed according to Neighbor-Joining by using MEGA
347 7.0 software (Kumar *et al.*, 2008).

348 The greenhouse microcosm experiment, consisting of dominant and companion
349 plants with and without mycorrhizal inoculum was performed at the Lhasa
350 agroecological experiment station (29°40'N, 91°20'E, 3688 m above sea level) in July
351 2019. Each pot (height: 45 cm, diameter: 32 cm) was filled with 2.0 kg of substrate
352 mixed with soil collected from nearby meadows and river sand (1:1, V/V), and steam-
353 autoclaved twice (1 day interval, 121 °C for 2 hours). Fresh soil collected from the
354 aforementioned meadow plots were used as mycorrhizal inoculums (40 g per pot),
355 which was added into the center of the autoclaved substrate soil in each pot. In
356 addition, 40 g of corresponding sterilized soil inoculum was added to create the non-
357 mycorrhizal treatment (NM, 4 replications). To correct for the differences in
358 communities of other non-AM fungi soil microbe, a soil microbial wash treatment was
359 applied to each NM pot, and it was prepared according to Jiang *et al.* (2018). We
360 blended 40 g of living-soil inoculum in 200 ml water, passed it through a 38 µm sieve,
361 and added the soil filtrate to each NM pot.

362 For transplantation of dominant and companion plants, three individuals of
363 either dominant or companion plant were collected at an early growth stage with the
364 same height from the corresponding degradation plots. Prior to transplantation, the
365 roots were washed and sterilized with 75% alcohol for 10 min. The main root of each
366 plant was retained, and the fine roots were cut off to eliminate the influence of
367 indigenous microorganisms. The three individuals of dominant or companion plant
368 were transplanted into pot separately, and 10 days later, the seedlings were thinned
369 to one individual per pot. A total of 48 pots (three degradation stages × two plant
370 species × two inoculation types × four replicates) were grown in the greenhouse (day
371 25 °C, night 17 °C), watered every 2 days, and the location of pots was randomly

372 switched every week.

373 The in-growth bottles (8 cm high, 3 cm diameter, connected with a 10 cm syringe
 374 for $^{15}\text{NH}_4\text{Cl}$ injection) containing sterilized substrate were buried to a depth of 5-15 cm
 375 in soil and 5 cm away from the plants. The bottle mouth was covered by 30 μm mesh
 376 (allowing the hyphae to pass through, but not roots). We put the in-growth bottles
 377 with inclining at 45° to prevent leakage of $^{15}\text{NH}_4\text{Cl}$ labeling solution (Fig. 2a, b). We
 378 dissolved 2 mg of $^{15}\text{NH}_4\text{Cl}$ in deionized water (i.e., 99 atom% ^{15}N , applied 1 mL of 2
 379 mg/mL) with a nitrification inhibitor (3,4-dimethyl pyrazole phosphate) that inhibits
 380 the transformation of $\text{NH}_4^+\text{-N}$ to $\text{NO}_3^-\text{-N}$ (Zerulla *et al.*, 2001). The ^{15}N isotope labeling
 381 was performed in the AM treatment, and the same corresponding amount of $^{14}\text{NH}_4\text{Cl}$
 382 was in the NM treatment.

383 The target plant was covered with a $^{13}\text{CO}_2$ pulse-labeling chamber (30 cm high,
 384 12 cm diameter) with a 5 mm pinhole at the top (Fig. 2a, b). We applied pulse labeling,
 385 i.e., 20 ml of $^{13}\text{CO}_2$ (99 atom% ^{13}C) through the pinhole every 2 hours 3 times, and
 386 sealed the pinhole immediately after each labeling. At midday, the AM inoculated
 387 plants were labeled with $^{13}\text{CO}_2$ for 6 hours. Correspondingly, the non-mycorrhizal
 388 plants were placed in the open air. The plants and in-growth bottles were destructively
 389 harvested 3 days after isotope labeling (Koegel *et al.*, 2013).

390 After 14 weeks, all individual plants were harvested to determine the ^{15}N
 391 concentration of the plant, and the ^{13}C concentration of AM fungal hypha. Plants were
 392 dried and ground into powder, and the ^{15}N concentration was determined using a
 393 Delta V Advantage isotope ratio mass spectrometer and an EA-HT element analyzer
 394 (Thermo Fisher Technology Company, USA). Soil PLFA extraction and ^{13}C -PLFA analysis
 395 from in-growth bottles were carried out according to Zhang's method (Zhang *et al.*,
 396 2019).

397 The concentrations of plant ^{15}N and AM fungal ^{13}C were calculated as follows:

398 Plant ^{15}N or AM fungal ^{13}C = $\text{T\%} \times (\text{atom\% AM} - \text{atom\% NM}) \times 100 / (99 - \text{atom\% NM})$

399 Where atom% AM is the atom percentage excess ^{15}N of plant or PLFA 16:1 ω 5c-
 400 ^{13}C of AM fungal hyphae in AM inoculated treatments, atom% NM is the mean atom

401 percentage excess ^{15}N of plant or PLFA 16:1 ω 5c- ^{13}C of AM fungal hyphae from four
402 randomly chosen NM treatments, and T% is the total N concentration of plant or C
403 concentration of AM fungal hyphae in AM inoculated treatments.

404 **Statistical analysis**

405 To estimate the effects of degradation and plant species on the currency in
406 exchanging plant C for AM fungal N, the concentration of AM fungal ^{13}C and plant ^{15}N ,
407 and the ratio of ^{13}C : ^{15}N were analyzed by linear mixed-effect models using the lmer
408 function in the lme4 package (Bates *et al.*, 2015), in which degradation was treated as
409 a fixed factor, and plant species as a random factor.

410 All statistical analyses were conducted using R v.4.1.3 (R Development Core Team,
411 2018). First, the normality and homoscedasticity of the data were determined by using
412 the Shapiro and Bartlett tests. When the data of soil properties, plant community
413 characteristics, isotope concentration, AM fungal community variables, and
414 morphological structure traits satisfied the assumption of homogeneity of variance, all
415 significant differences of these data were tested by analysis of variance (ANOVA)
416 followed by Tukey's honestly significant difference (HSD) at $P < 0.05$. If the data did not
417 satisfy the homogeneity assumption, a nonparametric Kruskal–Wallis test was carried
418 out by using the kruskal.test function in R.

419 To examine how correlations between AM fungal taxa change along a degradation
420 gradient, we conducted a co-occurrence network analysis using the igraph package
421 (Csárdi G *et al.*, 2024). The Spearman's correlation (Rho) coefficient between the
422 pairwise OTUs was inferred by the psych package with a threshold of FDR-adjusted P
423 < 0.05 and $r > |0.6|$ (Revelle, 2023). To visualize the variations in AM fungal community
424 composition, the AM fungal Bray–Curtis dissimilarity was subjected to PCo analysis
425 using the pcoa command in the ape package (Paradis *et al.*, 2004). The distance
426 matrices of the AM fungal community (Hellinger transformed) were calculated by
427 Bray–Curtis dissimilarity using the vegdist command in the vegan package (Clarke *et*
428 *al.*, 2006). Permutational analysis of variance (PERM ANOVA) was carried out to assess
429 the effect of compartment (root v.s. soil), degradation stage, and the interaction

430 between them on Bray–Curtis dissimilarities using the `adonis` command in `vegan`
431 package (Oksanen J *et al.*, 2022).

432 To explore the distribution of root and soil AM fungal taxa recovered from the
433 non- degraded, moderately degraded and severely degraded meadow root and soil
434 samples, we plotted ternary diagrams using the `ggtern` package (Hamilton & Ferry,
435 2018). In addition, we conducted indicator species analysis of AM fungal OTUs for each
436 degradation using the `indval` function in the `labdsv` package with the indicator values
437 (`indval`) and $P < 0.05$ (Roberts, 2023). To test the homogeneity of the AM fungal
438 community in root and soil along a degradation gradient, the beta-dispersion of AM
439 fungal communities was explored with the `betadisper` function in the `vegan` package
440 (Oksanen J *et al.*, 2022).

441

442 **Acknowledgments**

443 This study was financially supported by the National Natural Science Foundation of
444 China (32322053), the Second Tibetan Plateau Scientific Expedition and Research
445 (STEP) program (2019QZKK0304) and the Strategic Priority Research Program of the
446 Chinese Academy of Sciences (XDA2005010402).

447

448 **Competing interests**

449 None declared.

450

451 **Author contributions**

452 QD, BJ and YL conceived and designed the study. QD and SR conducted field,
453 greenhouse and laboratory work. QD performed the statistical analyses. QD wrote the
454 manuscript and CG gave critical revisions.

455

456 **Data availability**

457 Raw sequencing data have been deposited in the NCBI Sequence Read Archive under
458 accession no. [PRJNA1060898](https://www.ncbi.nlm.nih.gov/submit/sra/).

459 **References**

460

461 **Arguello A, O'Brien MJ, van der Heijden MG, Wiemken A, Schmid B, Niklaus PA. 2016.**462 Options of partners improve carbon for phosphorus trade in the arbuscular mycorrhizal
463 mutualism. *Ecology Letters* **19**(6): 648-656.464 **Babalola BJ, Li J, Willing CE, Zheng Y, Wang YL, Gan HY, Li XC, Wang C, Adams CA, Gao C,**465 **et al. 2022.** Nitrogen fertilisation disrupts the temporal dynamics of arbuscular
466 mycorrhizal fungal hyphae but not spore density and community composition in a
467 wheat field. *New Phytologist* **234**(6): 2057-2072.468 **Bai YF, Cotrufo MF. 2022.** Grassland soil carbon sequestration: Current understanding,
469 challenges, and solutions. *Science* **377**(6606): 603-608.470 **Bardgett RD, Bullock JM, Lavorel S, Manning P, Schaffner U, Ostle N, Chomel M, Durigan G,**471 **Fry EL, Johnson D, et al. 2021.** Combatting global grassland degradation. *Nature*
472 *Reviews Earth & Environment* **2**(10): 720-735.473 **Bates D, Mächler M, Bolker B, Walker S. 2015.** Fitting Linear Mixed-Effects Models Using lme4.
474 *Journal of Statistical Software* **67**(1): 1-48.475 **Bennett AE, Groten K. 2022.** The Costs and Benefits of Plant-Arbuscular Mycorrhizal Fungal
476 Interactions. *Annual Review of Plant Biology* **73**: 649-672.477 **Bowman RA. 1988.** A Rapid Method to Determine Total Phosphorus in Soils. *Soil Science*
478 *Society of America Journal* **52**(5): 1301-1304.479 **Bray RH, Kurtz LT. 1945.** Determination of total, organic, and available forms of phosphorus in
480 soils. *Soil Science* **59**(1): 39-46.481 **Breidenbach A, Schleuss PM, Liu S, Schneider D, Dippold MA, de la Haye T, Miede G,**482 **Heitkamp F, Seeber E, Mason-Jones K, et al. 2022.** Microbial functional changes mark
483 irreversible course of Tibetan grassland degradation. *Nature Communications* **13**(1):
484 2681.485 **Brooker RW, Maestre FT, Callaway RM, Lortie CL, Cavieres LA, Kunstler G, Liancourt P,**486 **Tielbörger K, Travis JM, Anthelme F, et al. 2007.** Facilitation in plant communities: the
487 past, the present, and the future. *Journal of Ecology* **96**(1): 18-34.488 **Brundrett M, Melville L, Peterson L. 1994.** *Practical methods in mycorrhiza research: based on*
489 *a workshop organized in conjunction with the Ninth North American Conference on*
490 *Mycorrhizae*: University of Guelph, Ontario, Canada.491 **Caporaso JG, Kuczynski J, Stombaugh J, Bittinger K, Bushman FD, Costello EK, Fierer N,**492 **Pena AG, Goodrich JK, Gordon JI, et al. 2010.** QIIME allows analysis of high-
493 throughput community sequencing data. *Nature Methods* **7**(5): 335-336.494 **Chagnon PL, Bradley RL, Klironomos JN. 2012.** Using ecological network theory to evaluate
495 the causes and consequences of arbuscular mycorrhizal community structure. *New*
496 *Phytologist* **194**(2): 307-312.497 **Charters MD, Sait SM, Field KJ. 2020.** Aphid Herbivory Drives Asymmetry in Carbon for498 Nutrient Exchange between Plants and an Arbuscular Mycorrhizal Fungus. *Current*
499 *Biology* **30**(10): 1801-1808.500 **Chaudhary VB, Holland EP, Charman-Anderson S, Guzman A, Bell-Dereske L, Cheeke TE,**501 **Corrales A, Duchicela J, Egan C, Gupta MM, et al. 2022.** What are mycorrhizal traits?
502 *Trends in Ecology & Evolution* **37**(7): 573-581.

- 503 **Che R, Wang Y, Li K, Xu Z, Hu J, Wang F, Rui Y, Li L, Pang Z, Cui X. 2019.** Degraded patch
504 formation significantly changed microbial community composition in alpine meadow
505 soils. *Soil and Tillage Research* **195**: 104426.
- 506 **Choi J, Summers W, Paszkowski U. 2018.** Mechanisms Underlying Establishment of Arbuscular
507 Mycorrhizal Symbioses. *Annual Review of Phytopathology* **56**: 135-160.
- 508 **Clarke KR, Somerfield PJ, Chapman MG. 2006.** On resemblance measures for ecological
509 studies, including taxonomic dissimilarities and a zero-adjusted Bray–Curtis coefficient
510 for denuded assemblages. *Journal of Experimental Marine Biology and Ecology* **330**(1):
511 55-80.
- 512 **Coban O, De Deyn GB, van der Ploeg M. 2022.** Soil microbiota as game-changers in
513 restoration of degraded lands. *Science* **375**(6584): abe0725.
- 514 **Csárdi G, Nepusz T, Traag V, Horvát Sz, Zanini F, Noom D MK. 2024.** igraph: Network Analysis
515 and Visualization in R. R package version 1.6.0. URL [https://CRAN.R-](https://CRAN.R-project.org/package=igraph)
516 [project.org/package=igraph](https://CRAN.R-project.org/package=igraph).
- 517 **Davidson J, Mathieson J, Boyne AW. 1970.** The use of automation in determining nitrogen by
518 the Kjeldahl method, with final calculations by computer. *Analyst* **95**(1127): 181-193.
- 519 **Davison J, Moora M, Öpik M, Adholeya A, Ainsaar L, Bâ A, Burla S, Diedhiou AG, Hiiesalu I,
520 Jairus T, et al. 2015.** Global assessment of arbuscular mycorrhizal fungus diversity
521 reveals very low endemism. *Science* **349**(6251): 970-973.
- 522 **de Vries FT, Griffiths RI, Knight CG, Nicolitch O, Williams A. 2020.** Harnessing rhizosphere
523 microbiomes for drought-resilient crop production. *Science* **368**(6488): 270-274.
- 524 **Dong Q, Guo X, Chen K, Ren S, Muneer MA, Zhang J, Li Y, Ji B. 2021.** Phylogenetic
525 Correlation and Symbiotic Network Explain the Interdependence Between Plants and
526 Arbuscular Mycorrhizal Fungi in a Tibetan Alpine Meadow. *Frontiers in Plant Science* **12**:
527 1-11.
- 528 **Dong SK, Shang ZH, Gao JX, Boone RB. 2020.** Enhancing sustainability of grassland
529 ecosystems through ecological restoration and grazing management in an era of
530 climate change on Qinghai-Tibetan Plateau. *Agriculture Ecosystems and Environment*
531 **287**: 1-16.
- 532 **Dorich RA, Nelson DW. 1983.** Direct Colorimetric Measurement of Ammonium in Potassium
533 Chloride Extracts of Soils. *Soil Science Society of America Journal* **47**(4): 833-836.
- 534 **Edgar RC. 2013.** UPARSE: highly accurate OTU sequences from microbial amplicon reads.
535 *Nature Methods* **10**(10): 996-1000.
- 536 **Gao C, Xu L, Montoya L, Madera M, Hollingsworth J, Chen L, Purdom E, Singan V, Vogel J,
537 Hutmacher RB, et al. 2022.** Co-occurrence networks reveal more complexity than
538 community composition in resistance and resilience of microbial communities. *Nature*
539 *Communications* **13**(1): 3867.
- 540 **Gibbs HK, Salmon JM. 2015.** Mapping the world's degraded lands. *Applied Geography* **57**: 12-
541 21.
- 542 **Hamilton NE, Ferry M. 2018.** ggtern: Ternary Diagrams Using ggplot2. *Journal of Statistical*
543 *Software* **87**(CN3): 1-17.
- 544 **Hammarlund SP, Harcombe WR. 2019.** Refining the stress gradient hypothesis in a microbial
545 community. *Proceedings of the National Academy of Sciences, USA* **116**(32): 15760-
546 15762.

- 547 **Harris RB. 2010.** Rangeland degradation on the Qinghai-Tibetan plateau: A review of the
548 evidence of its magnitude and causes. *Journal of Arid Environments* **74**(1): 1-12.
- 549 **Hernandez DJ, David AS, Menges ES, Searcy CA, Afkhami ME. 2021.** Environmental stress
550 destabilizes microbial networks. *The ISME Journal* **15**(6): 1722-1734.
- 551 **Hodge A, Helgason T, Fitter AH. 2010.** Nutritional ecology of arbuscular mycorrhizal fungi.
552 *Fungal Ecology* **3**(4): 267-273.
- 553 **Jiang SJ, Liu YJ, Luo JJ, Qin MS, Johnson NC, Opik M, Vasar M, Chai YX, Zhou XL, Mao L, et**
554 **al. 2018.** Dynamics of arbuscular mycorrhizal fungal community structure and
555 functioning along a nitrogen enrichment gradient in an alpine meadow ecosystem. *New*
556 *Phytologist* **220**(4): 1222-1235.
- 557 **Kakouridis A, Hagen JA, Kan MP, Mambelli S, Feldman LJ, Herman DJ, Weber PK, Pett-**
558 **Ridge J, Firestone MK. 2022.** Routes to roots: direct evidence of water transport by
559 arbuscular mycorrhizal fungi to host plants. *New Phytologist* **236**(1): 210-221.
- 560 **Kiers ET, Duhamel M, Beesetty Y, Mensah JA, Franken O, Verbruggen E, Fellbaum CR,**
561 **Kowalchuk GA, Hart MM, Bago A, et al. 2011.** Reciprocal rewards stabilize
562 cooperation in the mycorrhizal symbiosis. *Science* **333**(6044): 880-882.
- 563 **Koegel S, Boller T, Lehmann MF, Wiemken A, Courty P-E. 2013.** Rapid nitrogen transfer in the
564 Sorghum bicolor-Glomus mosseae arbuscular mycorrhizal symbiosis. *Plant signaling &*
565 *behavior* **8**(8): 1-3.
- 566 **Kumar S, Nei M, Dudley J, Tamura K. 2008.** MEGA: a biologist-centric software for evolutionary
567 analysis of DNA and protein sequences. *Briefings in Bioinformatics* **9**(4): 299-306.
- 568 **Li T, Cui L, Scotton M, Dong J, Xu Z, Che R, Tang L, Cai S, Wu W, Andreatta D, et al. 2022.**
569 Characteristics and trends of grassland degradation research. *Journal of Soils and*
570 *Sediments* **22**(7): 1901-1912.
- 571 **Li Y, Wang S, Jiang L, Zhang L, Cui S, Meng F, Wang Q, Li X, Zhou Y. 2016.** Changes of soil
572 microbial community under different degraded gradients of alpine meadow. *Agriculture,*
573 *Ecosystems and Environment* **222**: 213-222.
- 574 **Liu H, Wu Y, Xu H, Ai Z, Zhang J, Liu G, Xue S. 2021.** N enrichment affects the arbuscular
575 mycorrhizal fungi-mediated relationship between a C4 grass and a legume. *Plant*
576 *Physiology* **187**(3): 1519-1533.
- 577 **Lumini E, Orgiazzi A, Borriello R, Bonfante P, Bianciotto V. 2010.** Disclosing arbuscular
578 mycorrhizal fungal biodiversity in soil through a land-use gradient using a
579 pyrosequencing approach. *Environmental Microbiology* **12**(8): 2165-2179.
- 580 **Malik AA, Martiny JBH, Brodie EL, Martiny AC, Treseder KK, Allison SD. 2020.** Defining trait-
581 based microbial strategies with consequences for soil carbon cycling under climate
582 change. *The ISME Journal* **14**(1): 1-9.
- 583 **Mao L, Pan J, Jiang S, Shi G, Qin M, Zhao Z, Zhang Q, An L, Feng H, Liu Y. 2019.** Arbuscular
584 mycorrhizal fungal community recovers faster than plant community in historically
585 disturbed Tibetan grasslands. *Soil Biology and Biochemistry* **134**: 131-141.
- 586 **Martin FM, van der Heijden MGA. 2024.** The mycorrhizal symbiosis: research frontiers in
587 genomics, ecology, and agricultural application. *New Phytologist*: 1-21.
- 588 **Mcgonigle TP, Miller MH, Evans DG, Swan G. 1990.** A New Method which Gives an Objective
589 Measure of Colonization of Roots by Vesicular-Arbuscular Mycorrhizal Fungi. *New*
590 *Phytologist* **115**(3): 495-501.

- 591 **Norman RJ, Edberg JC, Stucki JW. 1985.** Determination of Nitrate in Soil Extracts by Dual-
 592 wavelength Ultraviolet Spectrophotometry. *Soil Science Society of America Journal*
 593 **49**(5): 1182-1185.
- 594 **Oksanen J, Simpson G, Blanchet F, Kindt R, Legendre P, Minchin P, O'Hara R, Solymos P,**
 595 **Stevens M, Szoecs E, et al. 2022.** vegan: Community Ecology Package. R package
 596 version 2.6-4. URL <https://CRAN.R-project.org/package=vegan>.
- 597 **Olsson PA, Baath E, Jakobsen I, Soderstrom B. 1995.** The use of phospholipid and neutral lipid
 598 fatty acids to estimate biomass of arbuscular mycorrhizal fungi in soil. *Mycological*
 599 *Research* **99**(5): 623-629.
- 600 **Opik M, Vanatoa A, Vanatoa E, Moora M, Davison J, Kalwij JM, Reier U, Zobel M. 2010.** The
 601 online database MaarjAM reveals global and ecosystemic distribution patterns in
 602 arbuscular mycorrhizal fungi (Glomeromycota). *New Phytologist* **188**(1): 223-241.
- 603 **Paradis E, Claude J, Strimmer K. 2004.** APE: Analyses of Phylogenetics and Evolution in R
 604 language. *Bioinformatics* **20**(2): 289-290.
- 605 **R Development Core Team. 2018.** *R: a language and environment for statistical computing,*
 606 *v.3.3.2.* Vienna, Austria: R foundation for Statistical Computing. URL [http://www.r-](http://www.r-project.org)
 607 [project.org](http://www.r-project.org).
- 608 **Revelle W. 2023.** psych: Procedures for Personality and Psychological Research. R package
 609 version 2.3.9. URL <https://CRAN.R-project.org/package=psych>.
- 610 **Roberts DW. 2023.** labdsv: Ordination and Multivariate Analysis for Ecology. R package version
 611 2.1-0. URL <https://CRAN.R-project.org/package=labdsv>.
- 612 **Sato K, Suyama Y, Saito M, Sugawara K. 2005.** A new primer for discrimination of arbuscular
 613 mycorrhizal fungi with polymerase chain reaction-denature gradient gel electrophoresis.
 614 *Grassland Science* **51**(2): 179-181.
- 615 **Selosse MA, Rousset F. 2011.** The Plant-Fungal Marketplace. *Science* **333**(6044): 828-829.
- 616 **Sims JR, Haby VA. 1971.** SIMPLIFIED COLORIMETRIC DETERMINATION OF SOIL ORGANIC
 617 MATTER. *Soil Science* **112**(2): 137-141.
- 618 **Smith SE, Read DJ. 2008.** *Mycorrhizal Symbiosis.* Cambridge, UK: Academic Press.
- 619 **Tian H, Gai JP, Zhang JL, Christie P, Li XL. 2009.** Arbuscular mycorrhizal fungi in degraded
 620 typical steppe of inner Mongolia. *Land Degradation and Development* **20**(1): 41-54.
- 621 **Tome E, Tagliavini M, Scandellari F. 2015.** Recently fixed carbon allocation in strawberry plants
 622 and concurrent inorganic nitrogen uptake through arbuscular mycorrhizal fungi. *Journal*
 623 *of Plant Physiology* **179**: 83-89.
- 624 **Van Geel M, Busschaert P, Honnay O, Lievens B. 2014.** Evaluation of six primer pairs targeting
 625 the nuclear rRNA operon for characterization of arbuscular mycorrhizal fungal (AMF)
 626 communities using 454 pyrosequencing. *Journal of Microbiological Methods* **106**: 93-
 627 100.
- 628 **Vetrovsky T, Kolarikova Z, Lepinay C, Awokunle Holla S, Davison J, Fleyberkova A, Gromyko**
 629 **A, Jelinkova B, Kolarik M, Kruger M, et al. 2023.** GlobalAMFungi: a global database of
 630 arbuscular mycorrhizal fungal occurrences from high-throughput sequencing
 631 metabarcoding studies. *New Phytologist* **240**(5): 2151-2163.
- 632 **Walder F, Niemann H, Natarajan M, Lehmann MF, Boller T, Wiemken A. 2012.** Mycorrhizal
 633 networks: common goods of plants shared under unequal terms of trade. *Plant*
 634 *Physiology* **159**(2): 789-797.

- 635 **Wang C, Yu QY, Ji NN, Zheng Y, Taylor JW, Guo LD, Gao C. 2023.** Bacterial genome size and
636 gene functional diversity negatively correlate with taxonomic diversity along a pH
637 gradient. *Nature Communications* **14**(1): 7437.
- 638 **Wright SF, Upadhyaya A. 1996.** Extraction of an abundant and unusual protein from soil and
639 comparison with hyphal protein of arbuscular mycorrhizal fungi. *Soil Science* **161**(9):
640 575-586.
- 641 **Wu H, Yang J, Fu W, Rillig MC, Cao Z, Zhao A, Hao Z, Zhang X, Chen B, Han X. 2022.**
642 Identifying thresholds of nitrogen enrichment for substantial shifts in arbuscular
643 mycorrhizal fungal community metrics in a temperate grassland of northern China. *New*
644 *Phytologist* **237**(1): 279-294.
- 645 **Zerulla W, Barth T, Dressel J, Erhardt K, Horchler von Locquenghien K, Pasda G, Rädle M,**
646 **Wissemeier A. 2001.** 3,4-Dimethylpyrazole phosphate (DMPP) - a new nitrification
647 inhibitor for agriculture and horticulture. *Biology and Fertility of Soils* **34**(2): 79-84.
- 648 **Zhang H, Ziegler W, Han X, Trumbore S, Hartmann H. 2015.** Plant carbon limitation does not
649 reduce nitrogen transfer from arbuscular mycorrhizal fungi to *Plantago lanceolata*. *Plant*
650 *and Soil* **396**(1-2): 369-380.
- 651 **Zhang YY, Zheng NG, Wang J, Yao HY, Qiu QF, Chapman SJ. 2019.** High turnover rate of free
652 phospholipids in soil confirms the classic hypothesis of PLFA methodology. *Soil Biology*
653 *and Biochemistry* **135**: 323-330.
- 654 **Zhu Q, Chen H, Peng C, Liu J, Piao S, He JS, Wang S, Zhao X, Zhang J, Fang X, et al. 2023.** An
655 early warning signal for grassland degradation on the Qinghai-Tibetan Plateau. *Nature*
656 *Communications* **14**(1): 6406.
- 657

658 **Figure Legends**

659

660 **Fig. 1 Meadow degradation promotes niche differentiation between root and soil**
661 **arbuscular mycorrhizal (AM) fungal communities. a** Bar graph showing the relative
662 abundance of AM fungal operational taxonomic units (OTUs) in root and soil along a
663 degradation gradient. **b** Principal coordinate (PCo) analysis of AM fungal community
664 Bray–Curtis dissimilarity with permutational analysis of variance (PERM ANOVA)
665 showing significant association of AM fungal community composition with
666 compartment, degradation stage, and their interaction. **c-d** Ternary plot
667 demonstrating the distribution of **c** root and **d** soil AM fungal indicator taxa detected
668 from the non-, moderately and severely degraded meadows. **c** Note we detected
669 biases for seven taxa of *Acaulospora* (1), *Claroideoglossum* (5), and *Rhizophagus* (1)
670 toward non-degraded meadow, and four taxa of *Glomus* toward moderately or
671 severely degraded meadows in root. **d** Five *Glomus* taxa exhibited significant bias
672 toward non-, moderately, or severely degraded meadows in soil. **e** Pairwise
673 dissimilarity between root and soil AM fungal community significantly increased from
674 non-, through moderately to severely degraded meadow. The P value above the
675 horizontal lines marked treatments in comparison, and the significance of difference
676 was tested by the Wilcoxon signed-rank test. **f** Beta-dispersion analysis showing that
677 the dissimilarity of AM fungal community was significantly higher in root than in soil
678 under moderately and severely degraded meadows, but not under non-degraded
679 meadow, as detected by the paired T-test at $P < 0.05$.

680

681 **Fig. 2 Meadow degradation increased the currency in exchanging carbon (C) for**
682 **nitrogen (N) between plants and arbuscular mycorrhizal (AM) fungi. a** The schematic
683 diagram of the in-growth bottles and $^{13}\text{CO}_2$ pulse-labeling chamber used in the isotope
684 labeling experiment. The in-growth bottles (8 cm high, 3 cm diameter, connected with
685 a 10 cm syringe for $^{15}\text{NH}_4\text{Cl}$ injection) containing sterilized substrate were buried to a
686 depth of 5-15 cm in soil and 5 cm away from the plants. The bottle mouth was covered
687 by 30 μm mesh (allowing the hyphae to pass through, but not roots). We put the in-
688 growth bottles with inclining at 45° to prevent leakage of $^{15}\text{NH}_4\text{Cl}$ labeling solution. The
689 $^{13}\text{CO}_2$ pulse-labeling chamber (30 cm high, 12 cm diameter) with a 5 mm pinhole at
690 the top covered the target plant for labeling $^{13}\text{CO}_2$. **b** Photo of experimental instrument
691 and plant. **c-d** The result of mixed-effect models showed that **c** the concentration of
692 ^{13}C detected in AM fungal hyphae was significantly lower in non-degraded meadow as
693 compared to the moderately and severely degraded meadows, whereas **d** the
694 concentration of ^{15}N detected in plants was not significantly affected by meadow
695 degradation. **e** The resource exchange currency as depicted by the ratio of $^{13}\text{C} : ^{15}\text{N}$ was
696 significantly higher in the moderately and severely degraded meadows, as compared
697 to that in the non-degraded meadow. The P value above the horizontal lines marked
698 treatments in comparison, and the significance of difference was tested by linear
699 mixed-effect models with the degradation as a fixed factor and plant identity as a
700 random factor.

701 **Fig. 3 Meadow degradation increased the co-occurrence network complexity of the**
702 **arbuscular mycorrhizal (AM) fungal community. a-c** The co-occurrence network of
703 AM fungal community in **a** non-degraded, **b** moderately degraded, and **c** severely
704 degraded meadows showed an increase in complexity with the increase of
705 degradation severity. Node colors in the co-occurrence network indicated the genera
706 of AM fungal taxa, and the edge colors represent positive (pink) and negative (blue)
707 associations. **d** The increase in the dominance of *Glomus* taxa to network complexity
708 with increasing meadow degradation level, as evidenced by the more than doubled
709 degree of *Glomus* taxa in the network of severely degraded meadow as compared to
710 that in the non-degraded meadow. **e-h** An increase in network complexity by meadow
711 degradation is evidenced by the doubling of **e** edge number, **f** connectance, **g** average
712 degree and **h** average clustering coefficient.

713

714 **Fig. 4 Meadow degradation increased arbuscular mycorrhizal (AM) fungal biomass**
715 **allocation to hyphae at the expense of spore. a-c** Analysis of variance (ANOVA)
716 showed that meadow degradation significantly **a** decreased AM fungal spore density
717 (SD, per gram of dry soil), **b** increased extraradical hyphal density (ERHD, per gram of
718 dry soil), and **c** increased intraradical colonization rate (IRCR, per 100 root fragments).
719 **d-f** Meadow degradation significantly **d** decreased the SD: ERHD ratio, **e** decreased the
720 SD: IRCR ratio, but **f** did not significantly influence the ERHD: IRCR ratio. Different
721 letters above the boxes indicated significant differences at $P < 0.05$ among the non-,
722 moderately and severely degraded meadows according to Tukey's honestly significant
723 difference or Kruskal–Wallis test. **g** A schematic diagram of the response of AM fungal
724 SD, ERHD and IRCR to meadow degradation. Note our findings suggest that meadow
725 degradation increased AM fungal biomass allocation to both the intra- and extra-
726 radical hyphae at the expense of spore.
727

728 **Supporting Information**

729 Additional Supporting Information may be found online in the Supporting Information
730 section at the end of the article.

731

732 **Fig. S1** Photographs of non-degraded, moderately degraded, and severely degraded
733 meadows in a Tibetan meadow.

734 **Fig. S2** The characteristics of plant community for non-degraded, moderately
735 degraded and severely degraded meadows in the field.

736 **Fig. S3** The properties of soil for non-degraded, moderately degraded and severely
737 degraded meadows in the field.

738 **Fig. S4** Rarefaction curve of AM fungal OTUs in root and soil along a degradation
739 gradient.

740 **Fig. S5** Phylogenetic tree of representative sequences of AM fungal OTUs obtained in
741 this study.

742 **Fig. S6** Pie chart of the relative abundance of AM fungal OTUs and sequencing reads.

743 **Fig. S7** Ternary plot of root and soil AM fungal indicator taxa detected from the non-,
744 moderately and severely degraded meadows.

745 **Fig. S8** Frequency distributions of all correlations between AM fungal taxa as assessed
746 by Spearman's Rho.

747 **Fig. S9** Correlations between AM fungal taxa in non-degraded, moderately degraded
748 and severely degraded meadows.

749

750 **Table S1** List of studies investigating the currency in exchanging C for nutrients (N; P)
751 between plant and AM fungi by isotope labeling technology.

752 **Table S2** List of studies investigating the changes of AM fungal biomass allocation.

Fig.1

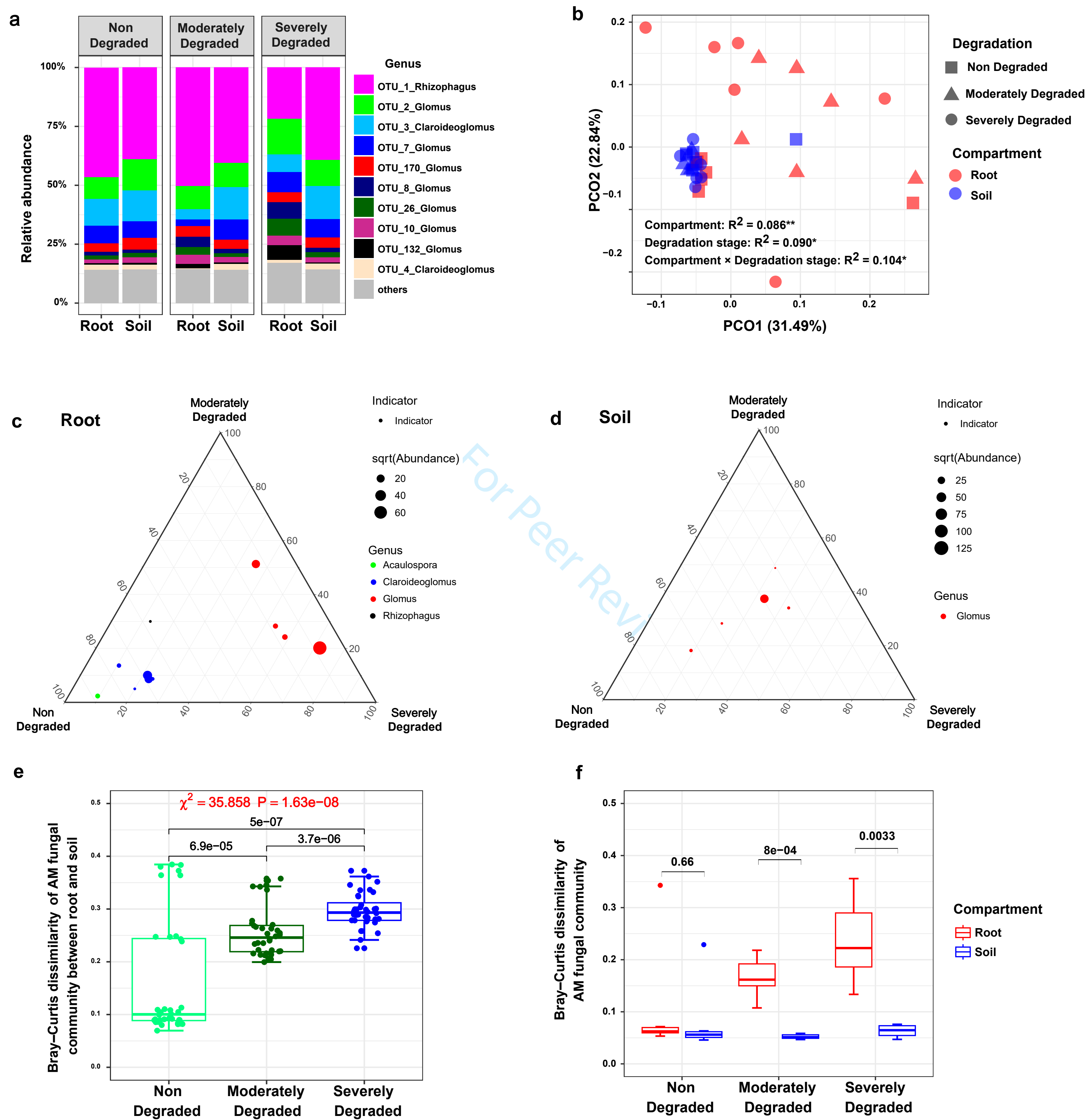
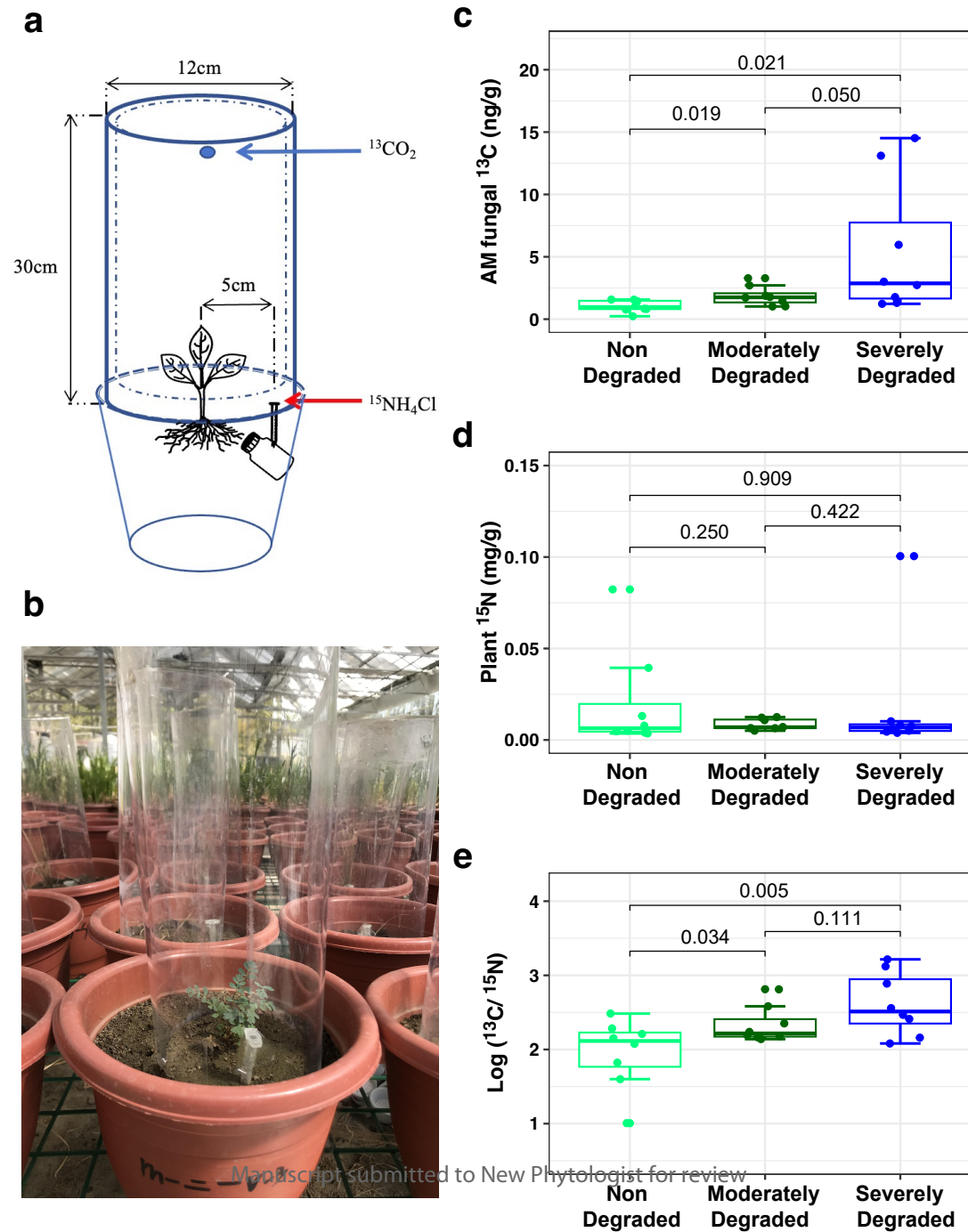
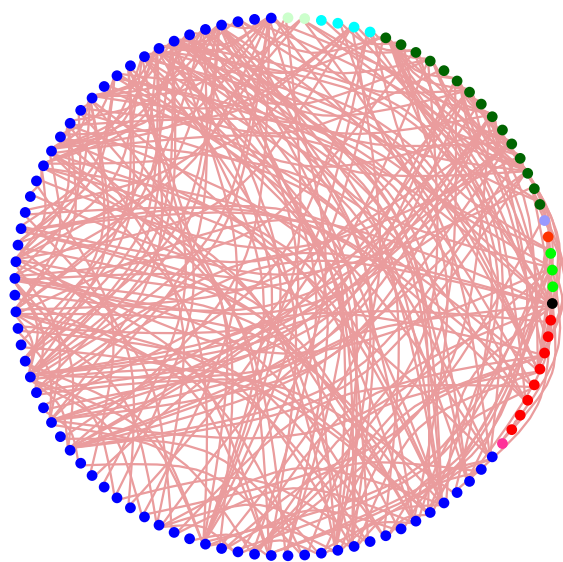


Fig.2



a Non-Degraded

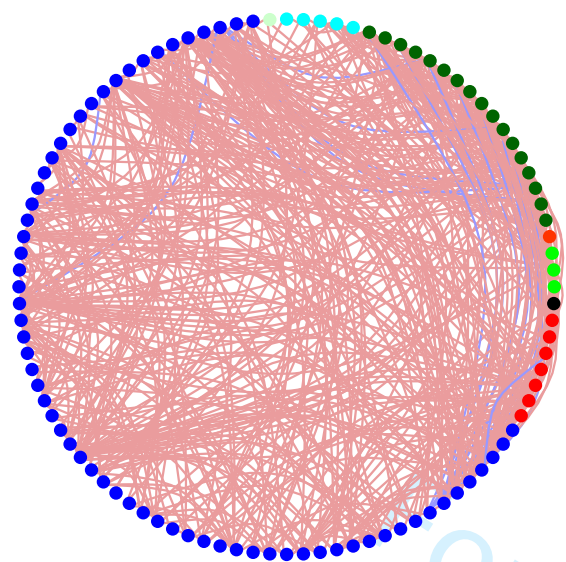
Positive links: 296
Negative links: 0



● Acaulospora ● Archaeospora ● Diversispora ● Glomus ● Rhizophagus — positive correlations
● Ambispora ● Claroideoglomus ● Funneliformis ● Paraglomus ● Scutellospora — negative correlations

b Moderately Degraded

Positive links: 493
Negative links: 18

**c Severely Degraded**

Positive links: 639
Negative links: 5

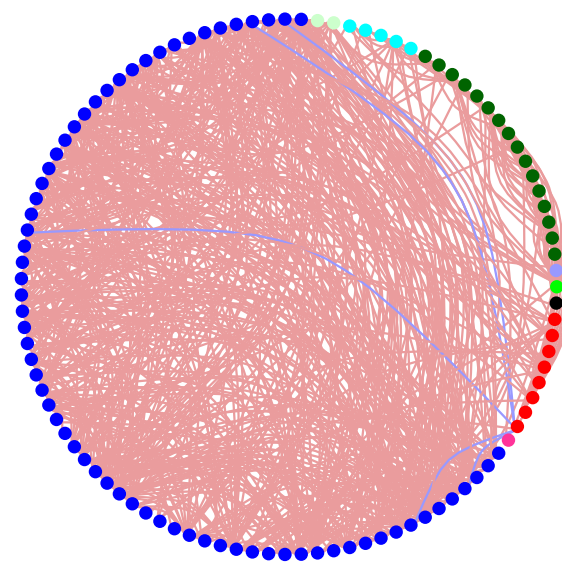


Fig.3

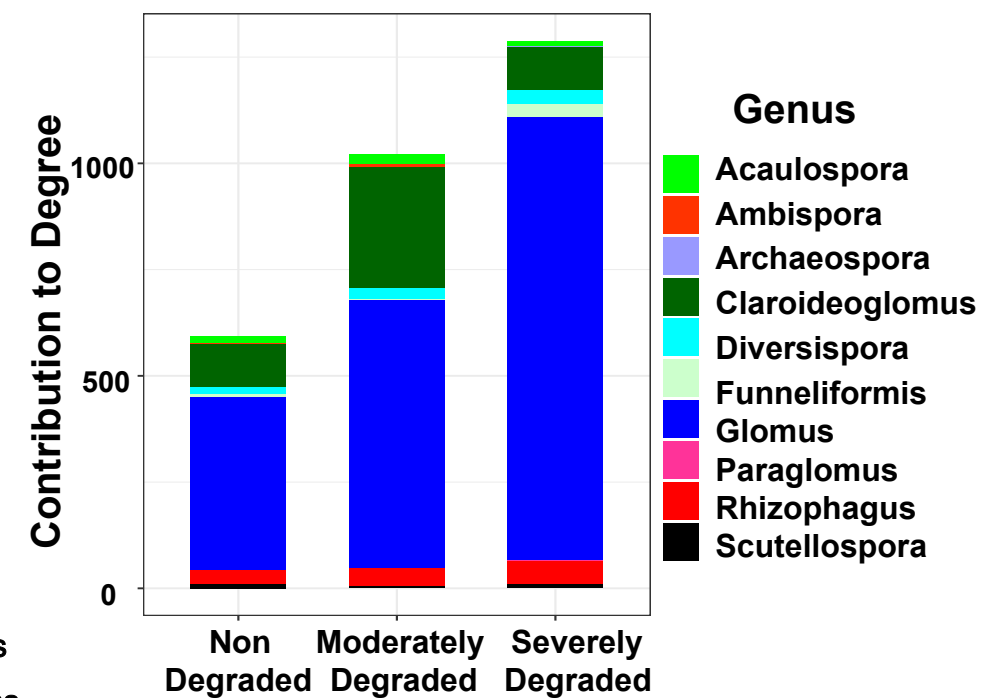
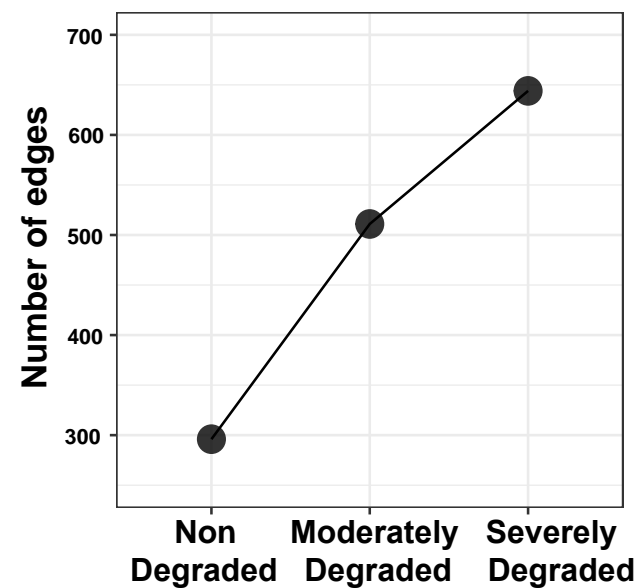
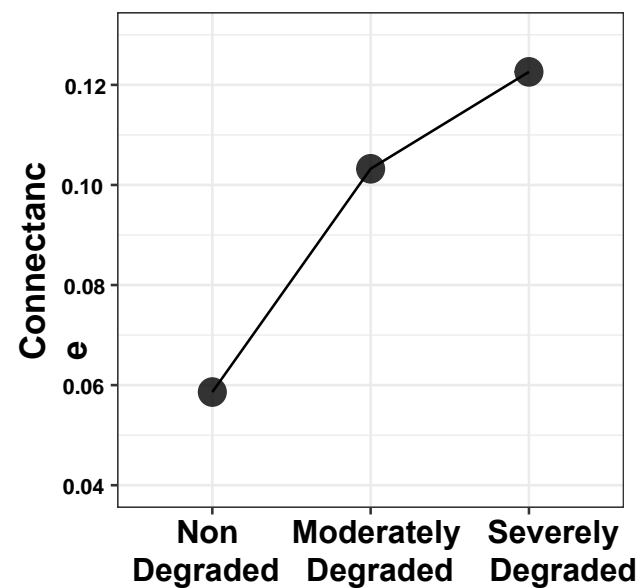
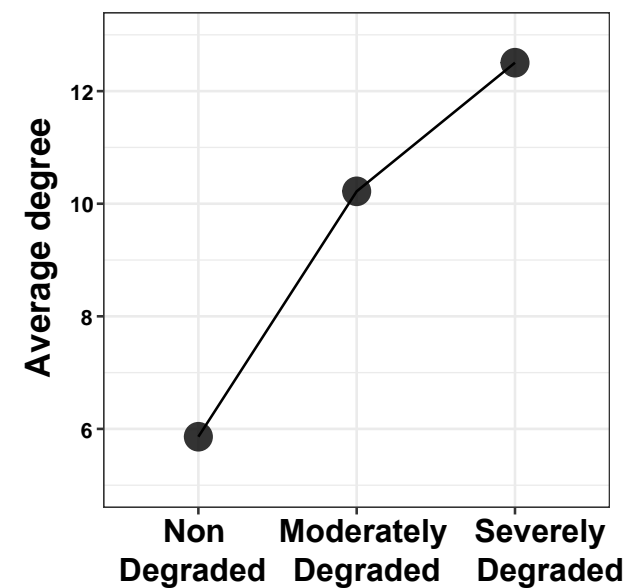
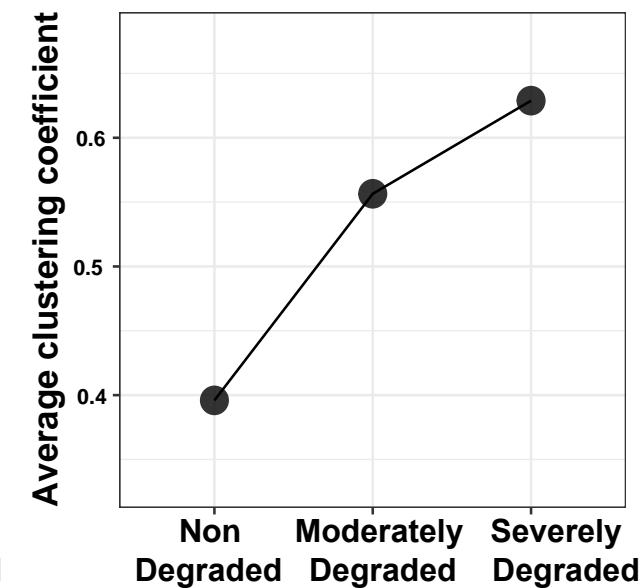
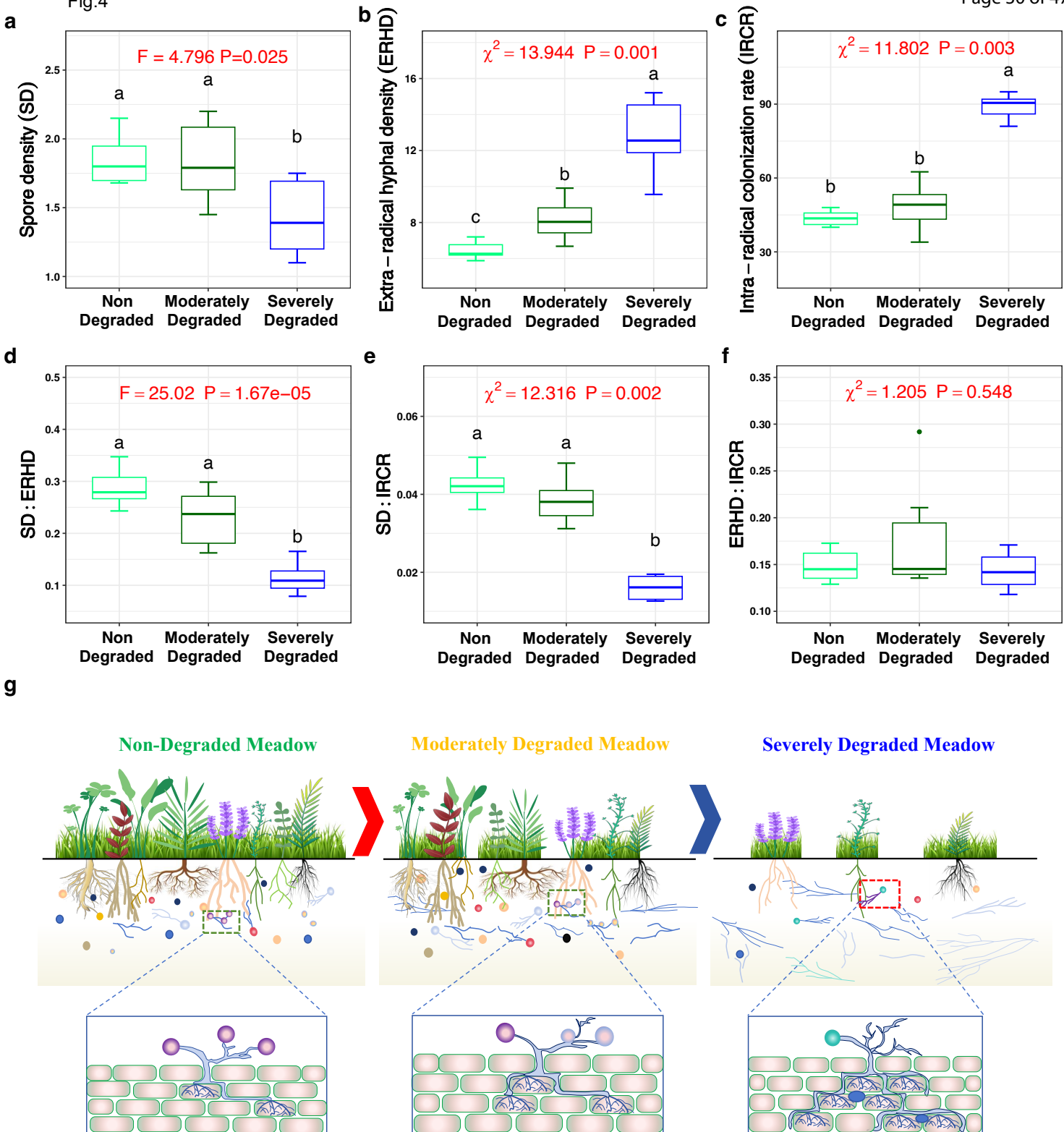
d**e****f****g****h**

Fig.4



1 **Article title:**

2 **Tibetan meadow degradation alters resource exchange currency, network**
3 **complexity, and biomass allocation tradeoff of arbuscular mycorrhizal symbiosis**

4
5 Qiang Dong^{1,2}, Shi-Jie Ren², Claire Elizabeth Willing³, Catharine Allyssa Adams^{4,5}, Yao-
6 Ming Li², Bao-Ming Ji^{2*}, Cheng Gao^{1,6*}

7
8 The following Supporting Information is available for this article:

9 **Fig. S1** Photographs of non-degraded, moderately degraded, and severely degraded
10 meadows in a Tibetan meadow.

11 **Fig. S2** The characteristics of plant community for non-degraded, moderately
12 degraded and severely degraded meadows in the field.

13 **Fig. S3** The properties of soil for non-degraded, moderately degraded and severely
14 degraded meadows in the field.

15 **Fig. S4** Rarefaction curve of AM fungal OTUs in root and soil along a degradation
16 gradient.

17 **Fig. S5** Phylogenetic tree of representative sequences of AM fungal OTUs obtained in
18 this study.

19 **Fig. S6** Pie chart of the relative abundance of AM fungal OTUs and sequencing reads.

20 **Fig. S7** Ternary plot of root and soil AM fungal indicator taxa detected from the non-,
21 moderately and severely degraded meadows.

22 **Fig. S8** Frequency distributions of all correlations between AM fungal taxa as assessed
23 by Spearman's Rho.

24 **Fig. S9** Correlations between AM fungal taxa in non-degraded, moderately degraded
25 and severely degraded meadows.

26
27 **Table S1** List of studies investigating the currency in exchanging C for nutrients (N; P)
28 between plant and AM fungi by isotope labeling technology.

29 **Table S2** List of studies investigating the changes of AM fungal biomass allocation.

30



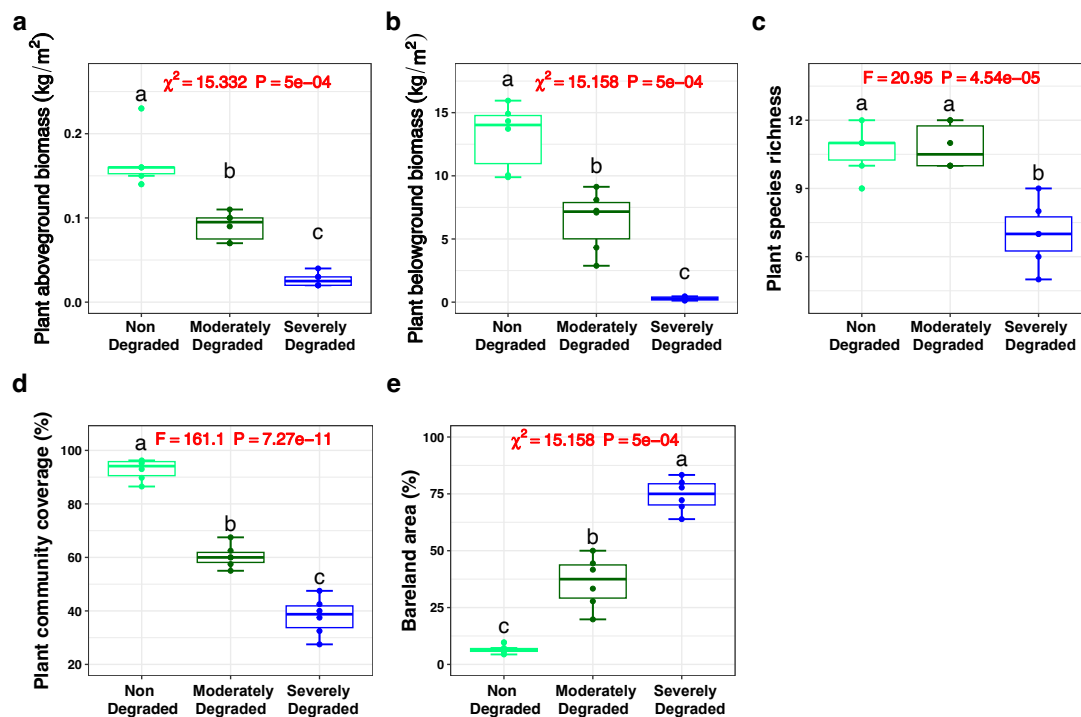
31

32 **Fig. S1** Photographs of non-degraded, moderately degraded, and severely degraded

33 meadows in a Tibetan meadow.

34

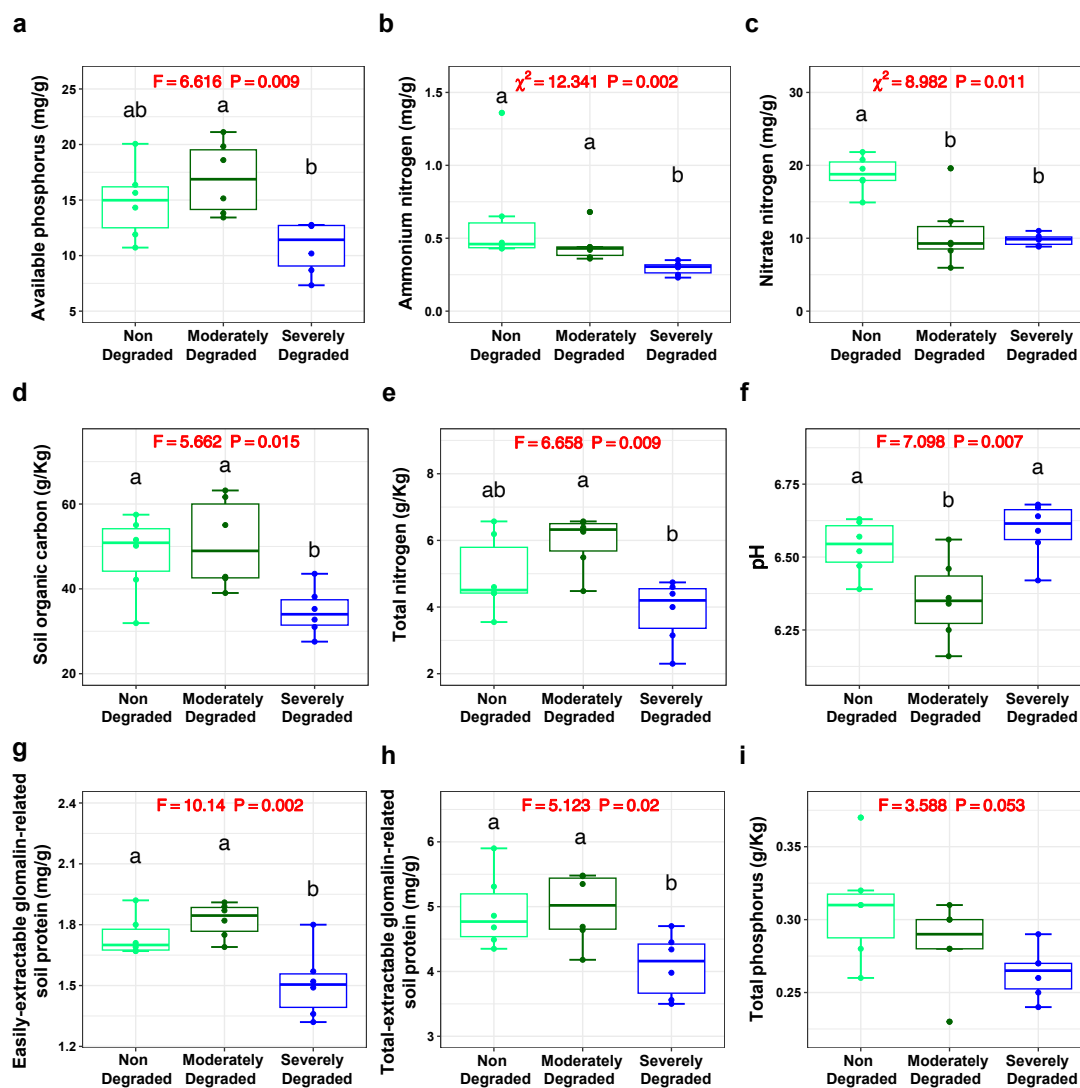
For Peer Review



35

36 **Fig. S2** The characteristics of plant community for non-degraded, moderately
 37 degraded and severely degraded meadows in the field (mean \pm SD, n = 6). The result
 38 of analysis of variance (ANOVA) and Kruskal–Wallis test showed that meadow
 39 degradation significantly decreased plant aboveground biomass, belowground
 40 biomass, species richness and community coverage, thereby increased bareland area.
 41 Different letters above the boxes indicated significant differences at $P < 0.05$ among
 42 the non-, moderately and severely degraded meadows according to Tukey's honestly
 43 significant difference or Kruskal–Wallis test.

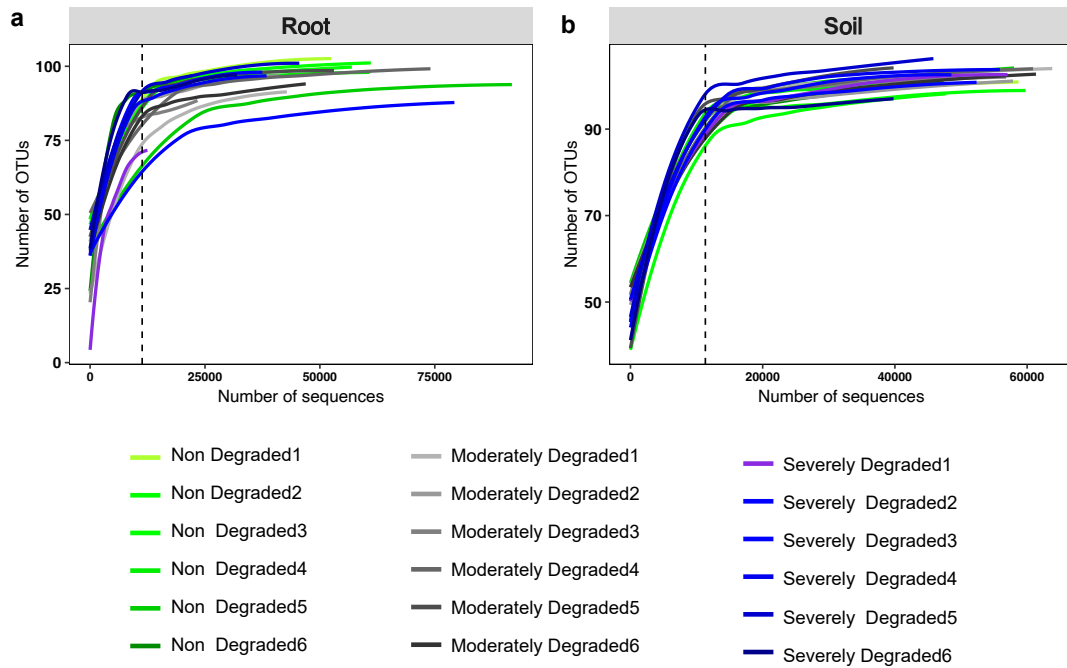
44



45

46 **Fig. S3** The properties of soil for non-degraded, moderately degraded and severely
 47 degraded meadows in the field (mean \pm SD, n = 6). The result of analysis of variance
 48 (ANOVA) and Kruskal–Wallis test showed that meadow degradation significantly
 49 affected soil available phosphorus (AP), ammonium nitrogen ($\text{NH}_4^+\text{-N}$), nitrate
 50 nitrogen ($\text{NO}_3^-\text{-N}$), soil organic carbon (SOC), total nitrogen (TN), pH, easily-extractable
 51 glomalin-related soil protein (EE-GRSP) and total-extractable glomalin related soil
 52 protein (T-GRSP), but not total phosphorus (TP). Different letters above the boxes
 53 indicated significant differences at $P < 0.05$ among non-, moderately and severely
 54 degraded meadows according to Tukey’s honestly significant difference or Kruskal–
 55 Wallis test.

56



57

58 **Fig. S4** Rarefaction curve of arbuscular mycorrhizal (AM) fungal operational taxonomic59 units (OTUs) in **a** root, **b** soil along a degradation gradient. The number of observed

60 OTUs was compared across samples when samples were rarefied at 11,329 sequences.

61



Glomeraceae

Acaulosporaceae

Gigasporaceae

Diversisporaceae

Claroideoglomeraceae

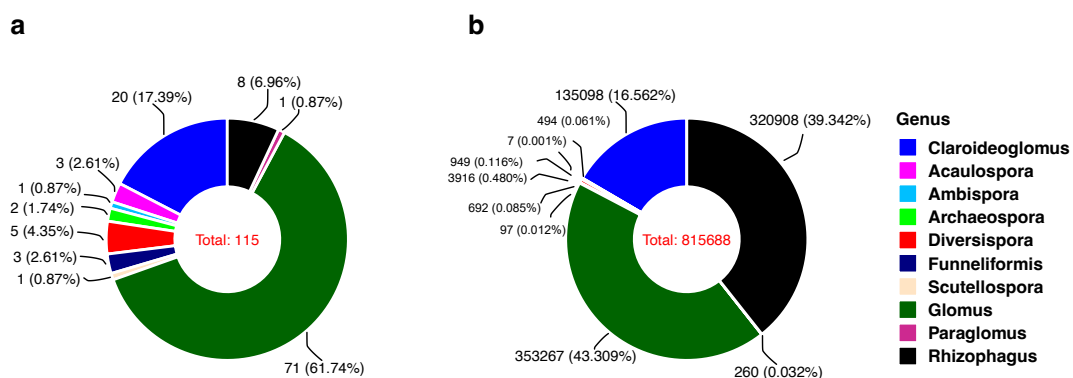
Archaeosporaceae

Ambisporaceae

Paraglomeraceae

63 **Fig. S5** Phylogenetic tree of representative sequences of arbuscular mycorrhizal (AM)
64 fungal operational taxonomic units (OTUs) obtained in this study with referenced
65 sequences from the National Center for Biotechnology Information (NCBI) and
66 MarrjAM database (<http://maarjam.botany.ut.ee>).
67

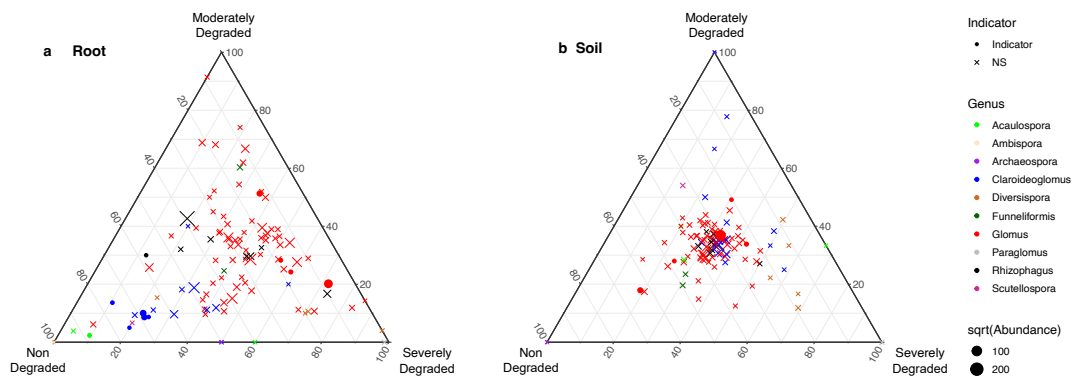
For Peer Review



68

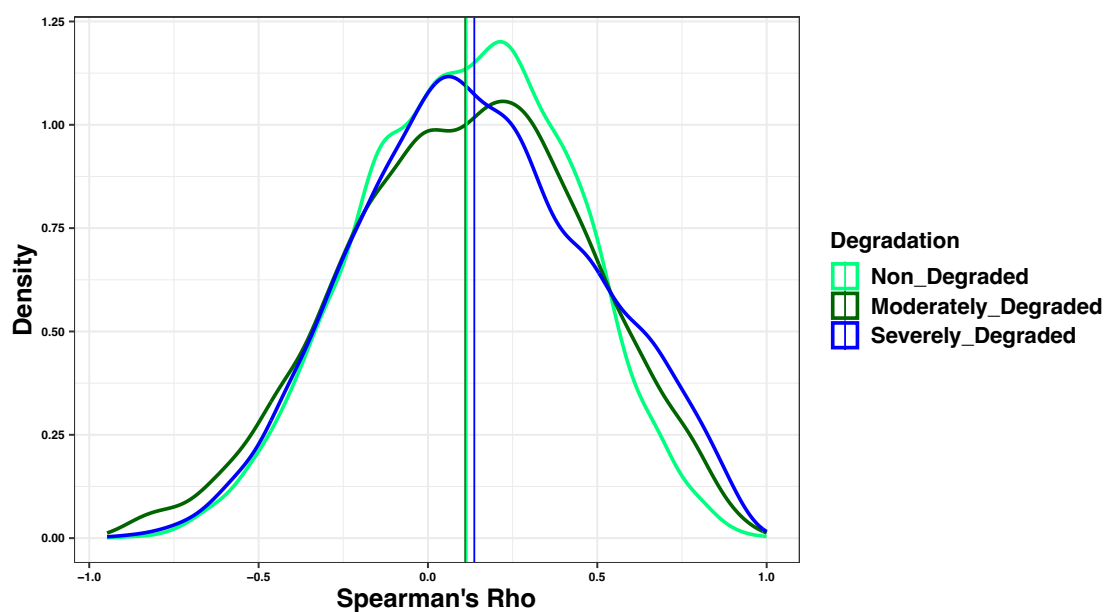
69 **Fig. S6** The pie graphs showed that the relative abundance of detected arbuscular
 70 mycorrhizal (AM) fungal genera **a** operational taxonomic units (OTUs) and **b**
 71 sequencing reads dominated by *Glomus*, *Claroideoglossum* and *Rhizophagus*.

72



73

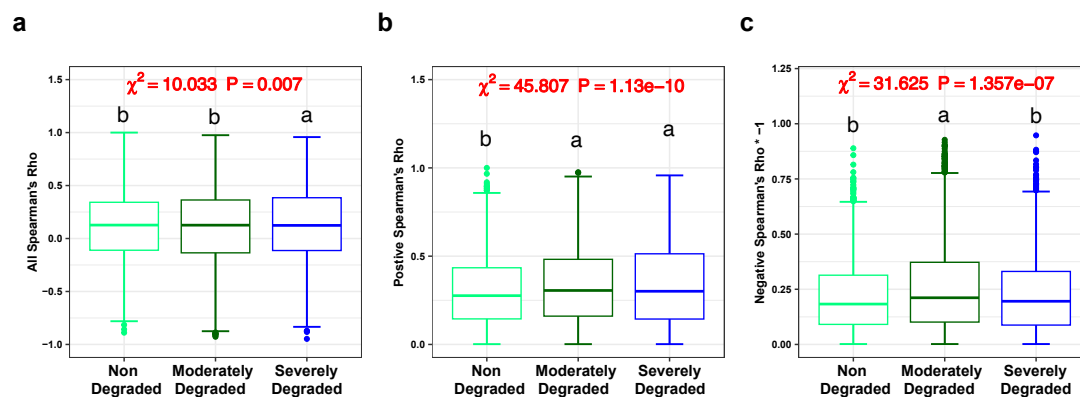
74 **Fig. S7** Ternary plot demonstrating the distribution of **c** root and **d** soil AM fungal
 75 indicator taxa detected from the non-, moderately and severely degraded meadows.
 76 **a** Note we detected biases for seven taxa of *Acaulospora* (1), *Claroideoglomus* (5), and
 77 *Rhizophagus* (1) toward non-degraded meadow, and four taxa of *Glomus* toward
 78 moderately or severely degraded meadows in root. **b** Five *Glomus* taxa exhibited
 79 significant bias toward non-, moderately, or severely degraded meadows in soil. Note
 80 ternary plots showed the distribution of both significant and non-significant (NS) AM
 81 fungal taxa detected from the non-, moderately and severely degraded meadows.



82

83 **Fig. S8** Frequency distributions of all correlations between arbuscular mycorrhizal (AM)
 84 fungal taxa as assessed by Spearman's Rho. Meadow degradation increased the
 85 proportion of correlations between AM fungal taxa.

86



87

88 **Fig. S9** Correlations between arbuscular mycorrhizal (AM) fungal taxa in non-degraded,
 89 moderately degraded and severely degraded meadows. **a-c** The result of Kruskal–
 90 Wallis test showed that meadow degradation significantly affected the all- correlation,
 91 positive correlation and negative correlation. **c** The positive correlation was
 92 significantly higher in the severely and moderately degraded meadows, as compared
 93 to the non-degraded meadow.

94

95 **Table S1** List of studies investigating the currency in exchanging carbon (C) for
 96 nutrients (nitrogen, N; phosphorus, P) between plant and arbuscular mycorrhizal (AM)
 97 fungi by isotope labeling technology.

Study	Ecosystem	Treatment	Exchange type	Change in currency	Conclusion
(Arguello <i>et al.</i> , 2016)	split-root system, greenhouse	AM fungal species identity and combination	Plant ^{14}C ~ AM fungal ^{33}P	*/*	Plants received more ^{33}P from less cooperative AM fungi in the presence of another AM fungal species
(Ji & Bever, 2016)	Split-root system, greenhouse	Phosphorus/ AM fungal species	Plant ^{14}C ~ AM fungal ^{32}P , and ^{33}P	NS/*	Host plant preferentially allocated more C to the roots associated with the fungus delivering higher P per unit plant C
(Zheng <i>et al.</i> , 2015)	split-root system	light/ AM fungal species	Plant ^{14}C ~ AM fungal ^{33}P	ND/ND	Plant preferential allocation towards the most beneficial mycorrhizal mutualist depends upon aboveground resources
(Williams <i>et al.</i> , 2017)	compartmented pot system	Nitrogen/ phosphorus	Plant ^{13}C ~ AM fungal ^{33}P	+/-	An alteration in the terms of P–C exchange under N fertilization regardless of soil P status
(Tome <i>et al.</i> , 2015)	compartmented pot system	Harvest time	Plant ^{13}C ~ AM fungal ^{15}N	+	The N uptake was linearly correlated with the ^{13}C fixed by the plants
(Gavito <i>et al.</i> , 2005)	Two compartment Petri dishes	Temperature / AM fungal species	root compartment D-glucose ^{13}C ~ hyphal ^{33}P	ND/ND	Root C uptake and translocation in the fungus were reduced by low temperatures. Uptake and translocation of ^{33}P by fungal hyphae were similar between 10 and 25°C.
(Hodge & Fitter, 2010)	compartmented pot system	Microcosm units/ AM fungal species/time	^{15}N / ^{13}C - labeled organic patch	ND/ND/ND	Substantial N acquisition by AM fungi from organic material
(Kiers <i>et al.</i> , 2011)	Triple-plate experiments	Phosphate supply/Sucrose supply/ AM fungal species	Root ^{14}C ~ hyphae ^{33}P	ND/ND/ <i>Glomus intraradices</i> > <i>Glomus aggregatum</i>	Host allocated more C (^{13}C) to more cooperative AM fungi than less cooperative AM fungal species

(Walder <i>et al.</i> , 2012)	compartmented pot system	Plant culture system/ AM fungal species	Root ¹³ C ~ hyphae ¹⁵ N / ³³ P	Sorghum (C4) > Flax (C3)/ Sorghum: <i>Glomus intraradices</i> < <i>Glomus mosseae</i> Flax: <i>Glomus intraradices</i> > <i>Glomus mosseae</i>	Sorghum (C4) invested more C in the AM fungi than flax (C3), but received less N and P from the AM fungi than did flax.
(Liu <i>et al.</i> , 2021b)	compartmented pot system	Plant culture system/ Nitrogen	hyphae ¹⁵ N / ¹³ C	ND	
(Liu <i>et al.</i> , 2021a)	compartmented pot system	Plant culture system/ phosphorus	hyphae ¹⁵ N / ¹³ C	ND	
(Charters <i>et al.</i> , 2020)	compartmented pot system	elevated CO ₂ / aphid herbivory	Plant ¹⁴ C ~ AM fungal ³³ P	ND	Insect herbivory drove asymmetry in C for nutrient exchange between symbionts
(Nuccio <i>et al.</i> , 2013)	compartmented pot system	AM fungus was permitted or excluded	¹³ C- and ¹⁵ N labeled root litter	ND	AM fungus significantly modifies the soil bacterial community and N cycling during litter decomposition
(Grabmaier <i>et al.</i> , 2014)	Greenhouse pots	Earthworms/ AM fungi	earthworms were dual-labeled with ¹⁵ N and ¹³ C	ND/ND	
(Xu <i>et al.</i> , 2018)	compartmented pot system	Phosphorus/ without or with AM fungi	Maize leaves dual-labeled with ¹⁵ N: ¹³ C	ND/ND	The host can acquire more nutrients through the AM from organic matter when soil P availability was low
(Zhang <i>et al.</i> , 2015)	glass growth chambers	ambient and low atmospheric CO ₂ /AM fungi	Plant ¹³ C ~ hyphae ¹⁵ N	ND/ND	Plant C limitation does not reduce N transfer from AM fungi to <i>Plantago lanceolata</i>
(Thirkell, Tom J. <i>et al.</i> , 2020)	compartmented pot system	ambient and elevated atmospheric CO ₂ / two barley cultivars	Plant ¹⁴ C ~ hyphae ¹⁵ N+ ³³ P	ND/ND	

(Thirkell, T. J. <i>et al.</i> , 2020)	compartmented pot system	ambient and elevated atmospheric CO ₂ /three wheat cultivars	Plant ¹⁴ C ~ hyphae ¹⁵ N+ ³³ P	ND/ND	C for nutrient exchange between AM fungi and wheat varies according to cultivar and changes in atmospheric C dioxide concentration
(Hoysted <i>et al.</i> , 2023)	in vitro monoxenic experimental system	intact fungi, trenched fungi and with no fungi present	Plant ¹⁴ C ~ hyphae ¹⁵ N+ ³³ P	ND	Clover gained both ¹⁵ N and ³³ P tracers directly from fungus in exchange for plant-fixed C in the absence of other micro-organisms
(Bever <i>et al.</i> , 2009)	split-root system,	AM fungal species identity and combination	Plant ¹⁴ C	ND	Host plants allocated more C toward the fungus that better promoted plant growth
(Hodge <i>et al.</i> , 2001)	compartmented pot system	without or with AM fungi	organic material with ¹³ C and ¹⁵ N	ND	AM fungus accelerates decomposition and acquires N directly from organic material

98 *, significant affect; +, significant increase; -, significantly decrease; NS, not significant;

99 ND, not done.

100

101 **Table S2** List of studies investigating the changes of arbuscular mycorrhizal (AM) fungal
 102 biomass allocation.

Study	Ecosystem	Treatment	SD: ERH	ERH: IRCR	SD: IRCR	Note
(Babalola <i>et al.</i> , 2022)	wheat field	Nitrogen / Water / Time	ND / ND / ND	* / * / *	ND / ND / ND	
(Johnson <i>et al.</i> , 2003)	Grassland	Nitrogen/s ite/season	ND / ND / ND	ND / ND / ND	ND / ND / ND	N enrichment impacts mycorrhizal allocation across a wide range of grassland ecosystems
(Weber <i>et al.</i> , 2019)	multi-factorial field experiment	global change drivers	ND	ND	ND	Glomeraceae, Claroideoglomeraceae and Paraglomeraceae as a rhizophilic guild that allocates more AM biomass to roots than soil, and the Gigasporaceae and Diversisporaceae as an edaphophilic guild that allocates more AM biomass to soil than roots
(Hart & Reader, 2002)	Conetainers culture	21 AM fungi isolates/ harvest dates/ four host plants	ND / ND / ND	ND / ND / ND	ND / ND / ND	The colonizing strategies of AM fungi differ considerably and that this variation is taxonomically based at the family level
(Mao <i>et al.</i> , 2019)	the Qinghai-Tibet highway from Xidatan to Amdo	Distance from highway	ND	ND	ND	The root length AM colonization in disturbed habitat was about twice that in undisturbed habitat, while inverse patterns were observed for the extraradical hyphal length density and spore density in soils

103 *, significant affect; NS, not significant; ND, not done.

104

- 105 **Arguello A, O'Brien MJ, van der Heijden MG, Wiemken A, Schmid B, Niklaus PA. 2016.**
 106 Options of partners improve carbon for phosphorus trade in the arbuscular mycorrhizal
 107 mutualism. *Ecology Letters* **19**(6): 648-656.
- 108 **Babalola BJ, Li J, Willing CE, Zheng Y, Wang YL, Gan HY, Li XC, Wang C, Adams CA, Gao C,**
 109 **et al. 2022.** Nitrogen fertilisation disrupts the temporal dynamics of arbuscular
 110 mycorrhizal fungal hyphae but not spore density and community composition in a
 111 wheat field. *New Phytologist* **234**(6): 2057-2072.
- 112 **Bever JD, Richardson SC, Lawrence BM, Holmes J, Watson M. 2009.** Preferential allocation to
 113 beneficial symbiont with spatial structure maintains mycorrhizal mutualism. *Ecology*
 114 *Letters* **12**(1): 13-21.
- 115 **Charters MD, Sait SM, Field KJ. 2020.** Aphid Herbivory Drives Asymmetry in Carbon for
 116 Nutrient Exchange between Plants and an Arbuscular Mycorrhizal Fungus. *Current*
 117 *Biology* **30**(10): 1801-1808.
- 118 **Gavito ME, Olsson PA, Rouhier H, Medina-Penafiel A, Jakobsen I, Bago A, Azcon-Aguilar C.**
 119 **2005.** Temperature constraints on the growth and functioning of root organ cultures
 120 with arbuscular mycorrhizal fungi. *New Phytologist* **168**(1): 179-188.
- 121 **Grabmaier A, Heigl F, Eisenhauer N, van der Heijden MGA, Zaller JG. 2014.** Stable isotope
 122 labelling of earthworms can help deciphering belowground–aboveground interactions
 123 involving earthworms, mycorrhizal fungi, plants and aphids. *Pedobiologia* **57**(4-6): 197-
 124 203.
- 125 **Hart MM, Reader RJ. 2002.** Taxonomic basis for variation in the colonization strategy of
 126 arbuscular mycorrhizal fungi. *New Phytologist* **153**(2): 335-344.
- 127 **Hodge A, Campbell CD, Fitter AH. 2001.** An arbuscular mycorrhizal fungus accelerates
 128 decomposition and acquires nitrogen directly from organic material. *Nature* **413**(6853):
 129 297-299.
- 130 **Hodge A, Fitter AH. 2010.** Substantial nitrogen acquisition by arbuscular mycorrhizal fungi from
 131 organic material has implications for N cycling. *Proceedings of the National Academy of*
 132 *Sciences, USA* **107**(31): 13754-13759.
- 133 **Hoysted GA, Field KJ, Sinanaj B, Bell CA, Bidartondo MI, Pressel S. 2023.** Direct nitrogen,
 134 phosphorus and carbon exchanges between Mucoromycotina 'fine root endophyte'
 135 fungi and a flowering plant in novel monoxenic cultures. *New Phytologist* **238**(1): 70-79.
- 136 **Ji B, Bever JD. 2016.** Plant preferential allocation and fungal reward decline with soil
 137 phosphorus: implications for mycorrhizal mutualism. *Ecosphere* **7**(5): 1-11.
- 138 **Johnson NC, Rowland DL, Corkidi L, Egerton-Warburton LM, Allen EB. 2003.** Nitrogen
 139 Enrichment Alters Mycorrhizal Allocation at Five Mesic To Semiarid Grasslands. *Ecology*
 140 **84**(7): 1895-1908.
- 141 **Kiers ET, Duhamel M, Beesetty Y, Mensah JA, Franken O, Verbruggen E, Fellbaum CR,**
 142 **Kowalchuk GA, Hart MM, Bago A, et al. 2011.** Reciprocal rewards stabilize
 143 cooperation in the mycorrhizal symbiosis. *Science* **333**(6044): 880-882.
- 144 **Liu H, Wu Y, Xu H, Ai Z, Zhang J, Liu G, Xue S. 2021a.** Mechanistic understanding of
 145 interspecific interaction between a C4 grass and a C3 legume via arbuscular mycorrhizal
 146 fungi, as influenced by soil phosphorus availability using a (13) C and (15) N dual-
 147 labelled organic patch. *The Plant Journal* **108**(1): 183-196.
- 148 **Liu H, Wu Y, Xu H, Ai Z, Zhang J, Liu G, Xue S. 2021b.** N enrichment affects the arbuscular

- 149 mycorrhizal fungi-mediated relationship between a C4 grass and a legume. *Plant*
 150 *Physiology* **187**(3): 1519-1533.
- 151 **Mao L, Pan J, Jiang S, Shi G, Qin M, Zhao Z, Zhang Q, An L, Feng H, Liu Y. 2019.** Arbuscular
 152 mycorrhizal fungal community recovers faster than plant community in historically
 153 disturbed Tibetan grasslands. *Soil Biology and Biochemistry* **134**: 131-141.
- 154 **Nuccio EE, Hodge A, Pett-Ridge J, Herman DJ, Weber PK, Firestone MK. 2013.** An arbuscular
 155 mycorrhizal fungus significantly modifies the soil bacterial community and nitrogen
 156 cycling during litter decomposition. *Environmental Microbiology* **15**(6): 1870-1881.
- 157 **Thirkell TJ, Campbell M, Driver J, Pastok D, Merry B, Field KJ. 2020.** Cultivar-dependent
 158 increases in mycorrhizal nutrient acquisition by barley in response to elevated CO₂.
 159 *Plants, People, Planet* **3**(5): 553-566.
- 160 **Thirkell TJ, Pastok D, Field KJ. 2020.** Carbon for nutrient exchange between arbuscular
 161 mycorrhizal fungi and wheat varies according to cultivar and changes in atmospheric
 162 carbon dioxide concentration. *Global Change Biology* **26**(3): 1725-1738.
- 163 **Tome E, Tagliavini M, Scandellari F. 2015.** Recently fixed carbon allocation in strawberry plants
 164 and concurrent inorganic nitrogen uptake through arbuscular mycorrhizal fungi. *Journal*
 165 *of Plant Physiology* **179**: 83-89.
- 166 **Walder F, Niemann H, Natarajan M, Lehmann MF, Boller T, Wiemken A. 2012.** Mycorrhizal
 167 networks: common goods of plants shared under unequal terms of trade. *Plant*
 168 *Physiology* **159**(2): 789-797.
- 169 **Weber SE, Diez JM, Andrews LV, Goulden ML, Aronson EL, Allen MF. 2019.** Responses of
 170 arbuscular mycorrhizal fungi to multiple coinciding global change drivers. *Fungal*
 171 *Ecology* **40**: 62-71.
- 172 **Williams A, Manoharan L, Rosenstock NP, Olsson PA, Hedlund K. 2017.** Long-term
 173 agricultural fertilization alters arbuscular mycorrhizal fungal community composition and
 174 barley (*Hordeum vulgare*) mycorrhizal carbon and phosphorus exchange. *New*
 175 *Phytologist* **213**(2): 874-885.
- 176 **Xu J, Liu S, Song S, Guo H, Tang J, Yong JWH, Ma Y, Chen X. 2018.** Arbuscular mycorrhizal
 177 fungi influence decomposition and the associated soil microbial community under
 178 different soil phosphorus availability. *Soil Biology and Biochemistry* **120**: 181-190.
- 179 **Zhang H, Ziegler W, Han X, Trumbore S, Hartmann H. 2015.** Plant carbon limitation does not
 180 reduce nitrogen transfer from arbuscular mycorrhizal fungi to *Plantago lanceolata*. *Plant*
 181 *and Soil* **396**(1-2): 369-380.
- 182 **Zheng C, Ji B, Zhang J, Zhang F, Bever JD. 2015.** Shading decreases plant carbon preferential
 183 allocation towards the most beneficial mycorrhizal mutualist. *New Phytologist* **205**(1):
 184 361-368.
- 185